International Journal of Thermophysics (2021) 42:171
https://doi.org/10.1007/s10765-021-02921-x

Alternative Heat Transfer Enhancement Techniques for Latent Heat Thermal Energy Storage System: A Review

Selvaraj Jegadheeswaran[1] · Athimoolam Sundaramahalingam[2] · Sanjay D. Pohekar[3]

Received: 17 June 2021 / Accepted: 20 September 2021 / Published online: 29 September 2021

Abstract

Various enhancement techniques are proposed in the literature to alleviate heat transfer issues arising from the low thermal conductivity of the phase change materials (PCM) in latent heat thermal energy storage systems (LHTESS). The identified techniques include employment of fins, insertion of metal structures, addition of high conductivity micro/nanoparticles, micro-encapsulation, macro-encapsulation and cascaded PCMs arrangement. However, these conventional techniques tend to reduce the storage capacity as they generally add additional components/materials into the storage medium. On the other hand, if techniques such as direct contact heat exchange, ultrasonic vibration, electrohydrodynamics and movable PCM are employed, the storage volume would remain unaffected. Hence, the said techniques seem to have gained importance in PCM research in recent times. Although several review papers elaborating conventional techniques are available, none can be found on the aforementioned alternative class. Driven by the current scenario, this review paper intends to summarize past research on alternative heat transfer enhancement techniques employed for LHTESS. The critical analysis of the potential of each technique in enhancing the phase change heat transfer rate and their practical applicability are presented. Further, the present review evaluates relative merits/demerits and challenges/issues/limitations of these techniques to provide guidelines for future research.

Keywords Direct contact heat exchange · Dynamic melting · Electrohydrodynamics · PCMflux · Screw heat exchangers · Ultrasonic waves

Abbreviations

EHD	Electrohydrodynamics
HTF	Heat transfer fluid

✉ Selvaraj Jegadheeswaran
jdees.2002@gmail.com

Extended author information available on the last page of the article

LHTESS	Latent heat thermal energy storage system
PCM	Phase change material
SHX	Screw heat exchanger
SSHX	Scraped surface heat exchanger

1 Introduction

Substantial utilization of renewable energy sources like solar thermal energy and the development of waste heat recovery systems are given much attention to nullify the impact on the environment [1]. However, large-scale and effective utilization of solar thermal energy demands an energy storage system that is also required for waste heat recovery [2]. The widely employed class of storage system is the one which is known as latent heat thermal energy storage system (LHTESS). This class of storage system stores the thermal energy as latent heat through the phase change material (PCM). Although LHTESS is known for multiple advantages, including higher energy density and heat transfer nearly at constant temperature [3, 4], the practical application is still questionable. Unfortunately, the PCMs which are generally employed in LHTESS (except metals and metal alloys which are used for high-temperature applications like power generation in satellites) do not offer a higher heat transfer rate as the thermal conductivity of PCMs falls within the range of 0.1–2 $W{\cdot}mK^{-1}$ [5]. Hence, the attention of researchers has been towards heat transfer enhancement techniques over the past few decades [6–8], and literature reveals that the following techniques remain at the top in PCM research.

(1) Finned heat exchangers [9–12]
(2) Augmentation of thermal conductivity through
    (i) Metal structures (balls, rings) [13, 14]
    (ii) Metal/non-metal porous structures [5, 15–17]
    (iii) Expanded graphite/Graphene/Carbon materials of various forms [18–20]
    (iv) Nano forms of metals/metal oxides/non-metals [21–25]
(3) Micro-encapsulation of PCM [26–28]
(4) Macro-encapsulation of PCM [29–34]
(5) Cascaded PCMs [35–37]

A comprehensive review of the above conventional techniques can be found in Refs. [38–42]. Although the conventional techniques are successfully employed and encouraging outcomes are reported, it can be understood that each of the above techniques suffers from some serious drawbacks.

When fins are used, there is a reduction in storage capacity as the addition of fins effectively reduces the quantity of PCM in the system. Hence, the system compactness is under threat. Secondly, the overall weight and cost would be on the higher side. The above problems are also applicable if high conductivity stable structures are employed for promoting the thermal conductivity of PCMs. Further, such

structures, including fins in the PCM, could well have an adverse effect on natural convection in the PCM [43]. It should be noted that the natural convection in the PCM is the major governing factor of the melting process [38].

Micro-encapsulation of PCMs seems to be a difficult and time-consuming process. Moreover, the large-scale production of PCM micro-capsules by existing methods is not yet realized. In recent years, nanotechnology has been showing very good progress, and the use of high conductivity nanomaterials as thermal conductivity promoters for PCMs has drawn a lot of attention. However, the preparation of nano-PCM composites requires special care, which consumes a lot of energy and time. Again, the large-scale production of such composites is a challenge. Though nanomaterials improve the PCMs' thermal conductivity considerably, the effect on other thermo-physical properties may not be desirable, and thus, effective enhancement in heat transfer rate could be affected. More importantly, nanocomposites are unstable due to the settlement of nano additives and are very expensive.

Unlike micro-encapsulation, the PCM is encapsulated in a container with a greater than 5 mm dimension in macro-encapsulation [31]. In fact, macro-encapsulated PCMs can be prepared using simple and low-cost processes which is not possible for micro-encapsulation [32]. A variety of container shapes are proposed, including rectangular, cylindrical, spherical, pouches, etc. [29]. Although the container can be either plastic or metal, a high heat transfer rate requirement demands only metals. In any case, the compatibility between PCM and container material is critical for ensuring stability of PCM and its high thermal performance even after a substantial number of thermal cycles [31]. Nevertheless, in the case of metal containers, corrosion poses a serious challenge unless proper lacquer coating is employed [29]. Further, welding or soldering methods are not found suitable for sealing the capsules as the corrosion protection coatings are severely affected by the thermal impact of such methods. Hence, only mechanical methods are suitable, which are expensive. In general, macro-encapsulated PCMs tend to melt and solidify at the edges and hence, the storage and retrieval processes become slower.

The cascaded technique would be effective only if the selected combination of PCMs yields homogeneous phase change. The compatibility between different PCMs is also an issue. Further, the cascaded arrangement is found to be more effective in a finned system [36]. Once fins are integrated, it is obvious that PCM volume tends to reduce.

Hence, alternative techniques which should enhance the heat transfer rate in PCMs without suffering from the drawbacks associated with conventional techniques could be more viable. Accordingly, a relatively new class of techniques are identified and are gaining attention. Quite a number of such techniques are proposed in the literature, and the results are encouraging. However, the volume of research focusing on the above techniques appears to be less than those on conventional techniques proposed for PCMs. Furthermore, a good number of review papers elaborating conventional techniques are available, whereas none can be found on alternative techniques (except the one by Tay et al. [44], which summarizes the past works on few dynamic techniques).

In this perspective, this review aims to summarise the proposed alternative techniques for LHTESS by various researchers. A critical analysis of the practical

applicability of the techniques is presented. Further, the relative merits and demerits of each technique are evaluated to provide future research direction.

2 Alternative Heat Transfer Enhancement Techniques for PCMs

The following techniques are considered alternative techniques for enhancing the thermal performance of LHTESS as they do not demand additional materials or components in the storage medium.

(1) Direct contact heat exchange
(2) Ultrasonic vibration
(3) Electrohydrodynamics
(4) Movable PCM
  (i) Screw heat exchanger (SHX)
  (ii) Recirculation of PCM
  (iii) PCMflux
  (iv) Scraping of solidified layer

The succeeding sections deliberate on all the above techniques along with the related research and their outcomes.

3 Thermal Energy Storage by Direct Contact Heat Transfer

Direct contact heat exchangers are proved to be the most effective and inexpensive among all types of heat exchangers [45]. However, the practical applications are generally limited as the two fluids exchanging heat should be immiscible if they are liquids. Direct contact heat exchange between HTF and PCM in LHTESS results in higher charging and discharging rates. Further, the energy density is higher due to the absence of heat transfer pipes in the storage space [46]. In the case of LHTESS, it is possible to choose the appropriate PCM among the wide range of PCMs available depending on the type of heat transfer fluid (HTF). If water is HTF, as in the case of solar water heater, then PCMs like paraffin wax can be employed, whereas salt hydrates and erythritol are suitable for thermal oils found in industrial waste heat recovery systems [47–49]. Nevertheless, any class of PCM with a suitable melting point may not have a compatibility problem if the air is HTF (for example, solar air drier) [50, 51].

3.1 Direct Contact Fluid Mediums

Once the heat exchange between the two fluids is over, they must be separated. Unlike other heat transfer devices, the PCMs in LHTESS generally remain stationary, and the HTF flows in and out. Hence, the separation of fluids after the heat exchange is purely by the density difference between the two materials. If the density

of HTF is higher than that of PCM, the HTF is supplied from the top of the storage unit so that it can move down and flow out of the system from the bottom. On the other hand, HTF is to be supplied from the bottom, should PCM possess a higher density than HTF. Figure 1 shows the HTF flow direction with respect to the relative densities of HTF and PCM.

In the pioneering work by Etherington [52], a salt hydrate-mineral oil combination was used as PCM-HTF. In this case, the oil with a lower density than salt hydrate was supplied from the bottom. With the arrangement, the issues of subcooling and phase segregation could be significantly reduced. Further, enhanced thermal performance was observed during both charging and discharging processes.

After two decades, Edie et al. [53] and Edie et al. [54] employed salt hydrate (PCM) and a hydrocarbon fluid, namely Varsol (HTF). This combination also permits only upward distribution of HTF, and hence, it should be removed from the top. It is reported that the PCM was carried over by the HTF, which resulted in the deposit of solidified PCM in the HTF lines. In the later work by Costello et al. [55], three salt hydrates were tested with Varsol as HTF. The carry over of PCM was observed in this work also. However, it is further reported that an increase in HTF flow rate could minimize the carry over.

He and Setterwall [56] used paraffin wax as PCM and water as HTF. This is an appropriate combination for direct contact heat exchange because they are not only immiscible but also offer considerable density differences. Since the density of water is higher than that of paraffin wax, it was sprayed from the top of the 250 ml capacity tube, which served as a storage unit. It should be mentioned that the HTF is always allowed from the top, no matter whether it is the charging or discharging process.

During charging, the cold water (at a temperature below the melting point of PCM), which is sprayed continuously from the top, would go down through liquid due to its higher density. This results in an exchange of heat between PCM and HTF,

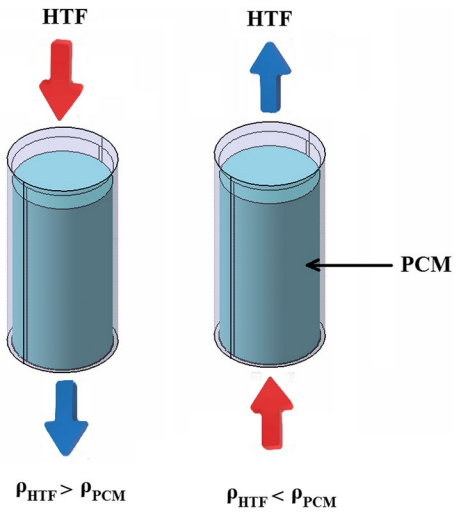

Fig. 1 Direction of HTF flow in a direct contact heat exchanger

and thus solidification takes place. Similarly, if water at a higher temperature than the melting point of PCM is sprayed into solid PCM, the top layer would get melted. This allows the water droplets to sink through, and further melting is established. Although it is mentioned that the direct contact system provides more effective heat transfer than conventional types, no heat transfer analysis is presented. However, the initial cost and operating cost were much lower as compared to conventional storage systems.

The extension work by Martin et al. [57] on a similar system provides much more insights into the thermal performance of direct contact storage. With optimum design variables (flow rate of HTF, temperature difference between HTF and PCM, and droplet size of HTF), high storage capacity and cooling power are possible to achieve. However, quite some practical issues are also highlighted. As the droplets of HTF sink through the PCM, solidification occurs around each droplet. In an ideal scenario, the out-flow rate of HTF should match with the in-flow rate. To accomplish this, all droplets covered by frozen PCM should collapse as they come down and allow the HTF to leave the system. In a practical scenario, this does not happen to all the particles, although some droplets may undergo the process towards the end. This obviously decreases the out-flow of the HTF during the majority of the period. Consequently, the HTF-PCM frozen bed keeps expanding downwards and may come out of the system if not prevented. The expansion is found to be higher at higher flow rates. Even at low flow rates, the problem of expansion still poses a problem. The authors have suggested employing a barrier kind of arrangement to force the droplets to collapse. However, the effectiveness of such an arrangement is not yet reported, which can be focused on in future studies.

During solidification, some quantity of liquid PCM gets trapped within the HTF/frozen PCM, which is porous. The trapped liquid PCM cannot get solidified as it is covered by solid PCM, which possesses very low thermal conductivity. This problem is observed at a higher temperature difference between HTF and PCM. This demands a trade-off between a high heat transfer rate and storage capacity.

3.2 Supply and Distribution of HTF

The key issue in direct contact LHTESS is the supply of HTF, which includes mode of admission and distribution. He and Setterwall [56] have mentioned that the HTF was sprayed from the top without reporting information on spraying device/distribution particles. However, the employment of multiple nozzles for better distribution of HTF sprayed from the top can be seen in literature [58]. On the other hand, Martin et al. [57] used distribution plates to ensure that the droplets are distributed all over. In any case, the spraying/distributing device does not come in contact with the PCM, and thus there will not be any issue of clogging by PCM crystals, whereas the device used to spray/distribute the lower density HTF from the bottom is subjected to plugging as it is generally surrounded by PCM.

Introducing and distributing HTF vertically upward from the bottom is the simplest way as the unit used does not need to run through the entire height of the storage container. Kiatsiriroat et al. [59] adopted a direct contact heat exchanger for the

evaporator to form ice. The refrigerant (HTF) was injected upward into water (PCM) stored in the container through an expansion device. Mulyono [60] also admitted HTF (kerosene) upward into salt hydrates using a distributor having holes of diameter 1/3/5 mm. Both Horibe et al. [61] and Naing et al. [62] used a nozzle plate located at the bottom to introduce oil in the upward direction. The nozzle plate is comprised of multiple holes to ensure better distribution of HTF. Similarly, Belusko et al. [63] distributed air through a perforated plate with 48 holes (each 1 mm diameter) to store cold energy in water. None of these works including the pioneer works given in Refs [53–55], has provided information on the clogging issue. However, Fouda et al. [64] experienced the said problem, which is quite apparent. Hence, it is important to address the clogging issue and to design a suitable distribution system for supplying HTF from bottom. On the other hand, quite some works have employed a distribution system that faces downward, although the designs vary from case to case [65–77].

As a simple technique, Fouda et al. [65] admitted HTF (Varsol) through a vertical pipe running from the top of the storage unit. The authors claim that the distribution and the heat transfer between HTF and PCM were satisfactory despite larger size HTF particles resulting from relatively larger diameter pipe. However, the HTF should be introduced in the form of fine particles of diameter as small as possible for better distribution and higher heat transfer rate. It is further recommended to position three pipes at different heights to pave alternate ways for HTF in case of a longer period shut down, resulting in clogging of the main pipe. Nevertheless, the problem associated with larger diameter pipes would remain, although the two additional pipes exist. In addition, this arrangement has the disadvantage of reduced PCM volume due to the space occupied by multiple pipes.

The more effective way of admitting HTF for better distribution and heat transfer rate could be using a multi-hole injection system. One such arrangement was employed by Kiatsiriroat et al. [66] to inject heat transfer oil into sodium thiosulphate pentahydrate. As far as the injection system is concerned, no details (number of injection holes, diameter) are revealed. Farid and Yacoub [70] and Farid and Khalaf [71] have provided the design details of the injection unit, which was basically a diffuser comprised of radially fitted eight glass tubes. The diameter of the tubes varied from 3 mm to 5 mm to get variable size HTF bubbles. Because of the radially arranged multiple holes, the distribution could have been better.

In the earlier work, Nomura et al. [72] used 9 holes of a 3 mm diameter injector (ring-shaped). From the results, the authors have identified that further smaller size holes and higher number of holes are worthwhile in augmenting heat transfer rate. In the subsequent work wherein a similar injection system was used, Nomura et al. [73] observed a drop in heat transfer rate at higher HTF flow rates. Of course, the heat transfer rate during melting and solidification in a direct contact system increases with an increase in-flow rate [60, 67, 74–77]. The diameter of the bubbles would be smaller when the flow rate is higher. The smaller diameter bubbles result in a higher heat transfer rate. Although the results of Nomura et al. [73] followed the trend mentioned above, it was only up to a specific value of flow rate. The drop in heat transfer rate at flow rates beyond a certain value was attributed to the non-uniform distribution of HTF.

In order to overcome the challenge mentioned above, an injection system with an increased number of holes having reduced diameter (18 holes, 2.5 mm diameter), was tested in the subsequent works [68, 69]. This proved effective as the system exhibited significant improvement in heat transfer rate even at higher flow rates which otherwise caused lower heat transfer rates. Hence, it is demonstrated that higher number and smaller diameter injection nozzles result in uniform distribution of HTF and thus no adverse effect on phase change processes at higher flow rates. The various designs of distribution systems employed are presented in Fig. 2.

3.3 Flow Channels for HTF

The introduction of HTF from the bottom faces another challenge no matter whether the injection system is positioned upward or downward. The HTF admitted can

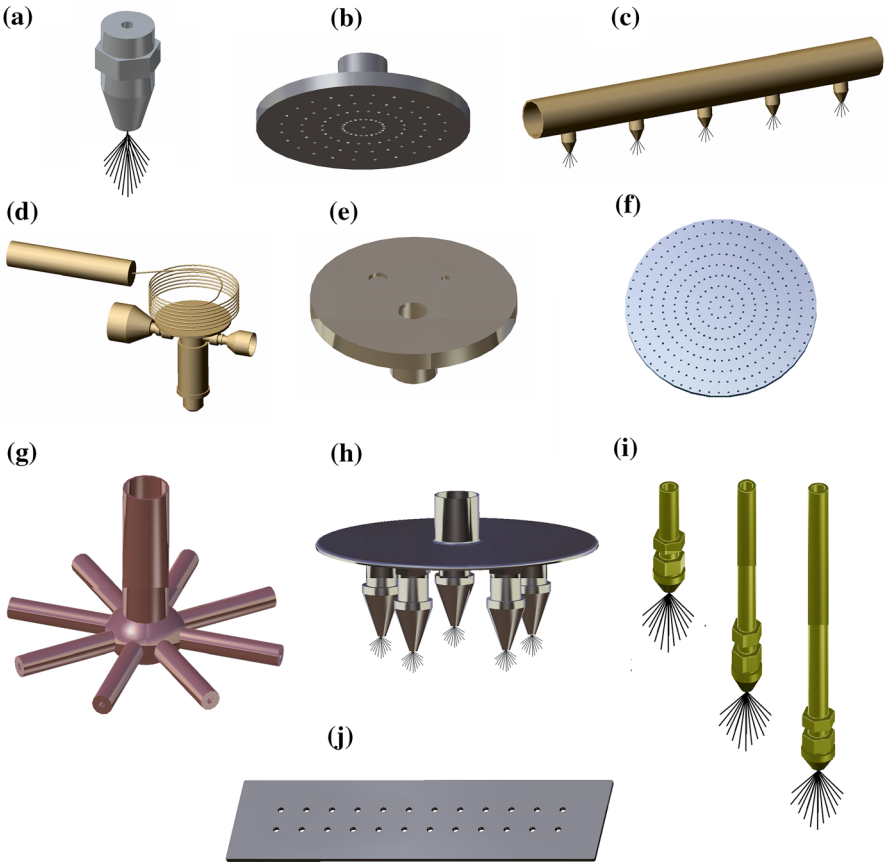

Fig. 2 Various designs of distribution systems employed in direct contact LHTESS (a) spray nozzle; (b) distributing plates; (c) multiple spraying nozzles; (d) expansion valve; (e) distributor plate with 3 holes of different diameters; (f) perforated plate; (g) diffuser comprises of radially fitted tubes; (h) multi-head injector; (i) three feed pipes located at different heights; (j) nozzle plate having 24 holes

easily pass through the liquid PCM during discharging, whereas during charging, the solid PCM obviously would block the HTF-free flow until a considerable amount of PCM gets melted. In other words, HTF can start flowing freely only after some time during which passages (channels) for HTF flow are formed [75]. According to Wang [78], the charging process was accelerated only after 90 min. This problem can be alleviated by establishing flow channels before HTF starts flowing, as suggested by Guo et al. [74]. The results from the simulation of melting in a cylindrical container have revealed that the flow channels in the solid PCM prior to HTF flow reduces the charging time by about 30 %.

In a physical system, Guo et al. [79] employed cuboid tubes (three in numbers) with three holes in each pipe. Cylindrical electrical heaters were stationed vertically in each hole in such a way that there is a small hole between each side of the heater and inlet pipe wall. These gaps act as nozzles for admitting HTF vertically (Fig. 3a). During charging, the heaters heat nearby PCM so that the melted quantity provides flow channels right from the beginning. The authors have reported that the formation of channels took only 90 s, and the initial and middle phases of charging were much faster compared to the heater-less system. With a similar arrangement, Gao et al. [80] have proved that the total melting time of erythritol-expanded graphite composite PCM could be reduced by 10 %. However, the amount of energy needed to operate such heaters should be taken into account. Although Guo et al. [79] observed only about 5 % of the stored energy as energy consumption in the tested system and have predicted that it would be even less in the case of real-time systems, further validation is required on this. In addition, the space occupied by electric heaters would reduce the effective storage volume.

Without electric heaters, the flow channels can still be established, as demonstrated by Wang et al. [81]. In this arrangement, the tubes with annular fins which carry the HTF were used to heat the PCM around the tubes (Fig. 3b). However, such arrangement demands a downward flow of HTF, and hence, the tubes have to run through from top to bottom. Although no energy is required in the absence of

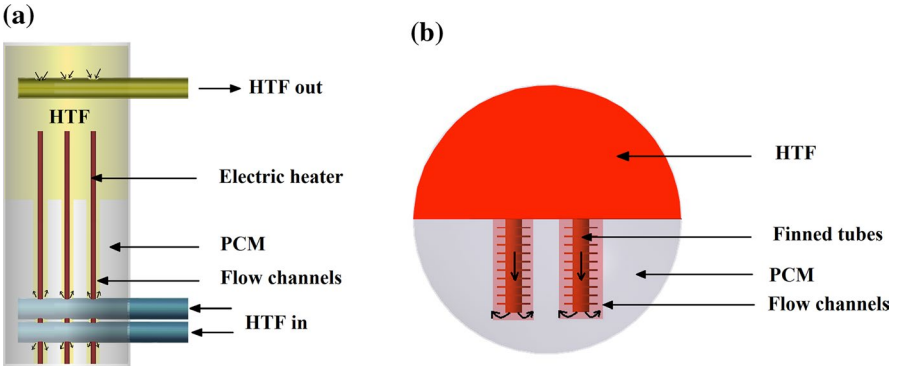

Fig. 3 Arrangements for the establishment of flow channels in direct contact heat exchanger (a) electric heaters [79]; (b) finned tubes [81]

electric heaters, the volume occupied by tubes, that too with fins, could be higher compared to the case employing electric heaters.

Although quite a number of investigations have focused on employing direct contact heat exchangers for LHTESS (The summary of those works is presented in Table 1), the full-scale practical application has not yet been witnessed as the technology is still under research [42].

3.4 Limitations

As mentioned earlier, effective direct contact heat exchange requires flow channels that demand power and space-consuming electric heaters or space-consuming finned tubes. Also, the distribution system may result in additional weight and cost. In addition, direct contact heat exchangers suffer from the following disadvantages:

Direct contact heat exchange can take place only if the interacting fluids are at the same pressure. Secondly, the insufficient density difference between the fluids would lead to the entrainment of one in the other, resulting in poor heat exchange. Similarly, if the degree of immiscibility is low, the system would experience mass transfer and chemical interaction issues, especially at high temperatures.

4 Ultrasonic Vibration

Vibration-based techniques can considerably increase heat transfer rate, and surface vibration technique has been tested on various heat transfer devices [82–87]. In surface vibration, the selected surface of the heat transfer device is made vibrating at low/high frequency to agitate the fluid. This results in bulk fluid mixing, which promotes convective heat transfer. The employment of surface vibration can also be seen in few works dealing with LHTESS [88–91]. Since it is difficult to make the surfaces of real-time systems vibrate, causing the fluid disturbance without bothering the device would be a viable alternate option practically. In this perspective, ultrasonic waves are found to be very effective.

Raben [92] demonstrated that heat transfer enhancement due to ultrasonic vibrations was considerable only when Reynolds number is low (absence of forced convection). Since natural convection is dominant during melting, ultrasonic waves would significantly impact the melting rate. Although conduction dominates the solidification process, ultrasonic effects can still be realized as long as a considerable amount of liquid PCM exists.

When ultrasonic waves (frequency above 20 kHz) propagate through a fluid, they cause intense agitation in the fluid. Besides agitating the fluid, the propagating waves result in a couple of critical effects, namely cavitation and acoustic streaming [93]. Acoustic cavitation is nothing but the formation of bubbles at low pressure and the collapse of bubbles at high pressure. The low and high-pressure cycles are caused by the propagation of ultrasonic waves in the liquid [94]. Acoustic streaming refers to a steady flow of bulk fluid due to the effect of energy absorption by the fluid from the ultrasonic wave [95]. Legay et al. [93] have also mentioned two other

Table 1 Summary of reported works on direct contact heat exchanger for LHTESS

References	PCM	HTF	Application	Nature of work	Highlights
Etherington [52]	Salt hydrate	Mineral oil	Heat storage	Experimental	Reduced subcooling and phase segregation Enhanced thermal performance during charging and discharging
Edie et al. [53]	Salt hydrate	Varsol	Solar energy storage	Experimental	Carry over of solid PCM by HTF Carry over results in salt deposition in heat exchanger
Costello et al. [55]	Salt hydrate	Varsol	Solar energy storage	Experimental	Increase in HTF flow rate reduces carry over of solid PCM
Kunkel et al. [46]	Eutectic mixture of magnesium nitrate hexahydrate and magnesium chloride hexahydrate	Mineral oil	Heat storage	Experimental	Optimal operating parameters are considered to prevent carry over of PCM Local heat transfer coefficient between the PCM and HTF is obtained using phase boundary surface between them
He and Setterwall [56]	Paraffin wax	Water	Cold storage	Experimental	Paraffin wax and water combination is proved to be better Direct contact system for cold storage is cost effective
Martin et al. [57]	Paraffin wax	Water	Cold storage	Theoretical and experimental	Influence of flow rate and temperature difference on storage capacity is reported Practical limitations are identified

Table 1 (continued)

References	PCM	HTF	Application	Nature of work	Highlights
Li et al. [58]	Organic PCM (HS-E2)	Air	Air-conditioning system	Numerical and experimental	Flow rate of liquid PCM influences the freezing time HTF inlet temperature has insignificant influence on charging capacity
Kiatsiriroat et al. [59]	Water	R12 & R22	Direct contact evaporator	Theoretical and experimental	Lumped model can figure out temperature of water and amount of ice formed Lower volume of water is suggested for higher heat transfer coefficient
Mulyono [60]	Na_2CO_3 $10H_2O$ solution	Kerosene	Heat storage	Theoretical and experimental	Influence of flow rate and bubble diameter of HTF on the volumetric coefficient of heat transfer/storage capacity are reported
Horibe et al. [61]	Erythritol	Silicon oil	Medium temperature waste heat recovery	Experimental	Perforated partition plates are introduced to control the packed height of PCM The said arrangement accelerates the melting process
Naing et al. [62]	Mixture of mannitol and erythritol	Heat transfer oil	Medium temperature waste heat recovery	Experimental	Role of perforated plates and aluminium fibres on controlling solidified height is studied Metal fibre is proved to be more effective

Table 1 (continued)

References	PCM	HTF	Application	Nature of work	Highlights
Belusko et al. [63]	Water	Air	Cold thermal storage	Experimental	Unity heat exchange effectiveness could be achieved through out the phase change process Pumping losses are significant
Fouda et al. [64]	Glauber's salt	Kerosene	Solar thermal energy storage	Numerical and experimental	Any type of distributor system suffers from plugging issue Three inlet pipes located at different heights are recommended
Fouda et al. [65]	Glauber's salt	Varsol	Solar thermal energy storage	Experimental	Output power can be controlled by controlling flow rate and inlet temperature of HTF Thermal efficiency exceeds 95 %
Kiatsiriroat et al. [66]	Sodium thiosulphate pentahydrate	Heat transfer oil	Heat storage	Theoretical and experimental	PCM is shown to be uniform during discharging HTF outlet temperature, PCM temperature and solid fraction are evaluated using lumped model
Farid and Yacoub [70]	Hydrated salts	Kerosene	Heat storage	Theoretical and experimental	Radially arranged 8 glass tubes served as diffuser and no blockage was experienced Higher flow rate of HTF is recommended for higher heat transfer coefficient

Table 1 (continued)

References	PCM	HTF	Application	Nature of work	Highlights
Farid and Khalaf [71]	Hydrated salts	Kerosene	Solar thermal energy storage	Experimental	Two columns filled with different PCMs having different crystallization temperature are connected in series The arrangement exhibits higher heat transfer rate and allows the system to operate for longer duration
Nomura et al. [72]	Erythritol	Heat transfer oil	Heat storage	Experimental	Optimum conditions for uniform HTF flow are arrived Uniform HTF flow rate results in higher effectiveness
Wang et al. [77]	Erythritol	Heat transfer oil	Heat storage	Experimental and numerical	Solidification rate is increased by increasing HTF flow rate and by decreasing the inlet temperature Higher flow rate and lower inlet temperature leads to high discharge efficiency

effects; the heating of fluid medium progressively by acoustic energy and the acoustic fountain caused by high-frequency waves. All these ultrasonic effects are illustrated in Fig. 4. The resultant of these effects and the agitation caused by ultrasonic waves is responsible for enhancing the heat transfer rate.

4.1 Phase Change Heat Transfer under Ultrasonic Vibration

Some authors report the application of ultrasonic waves for improving phase change heat transfer rate. Although the report by Fairbanks [96] may be considered a pioneer study, it is not comprehensive. However, the role of ultrasonic waves in melting rate enhancement was well demonstrated in this work. In the comprehensive study by Choi and Hong [97], it is reported that ultrasonic waves could not impact the onset of natural convection. Further, the system without ultrasonic vibration exhibited a higher heat transfer coefficient during the initial phase, which is conduction dominated. Nevertheless, the overall melting rate is proved to be significantly higher, and ultrasonic waves also influence solid PCM as agitation of solid PCM results in

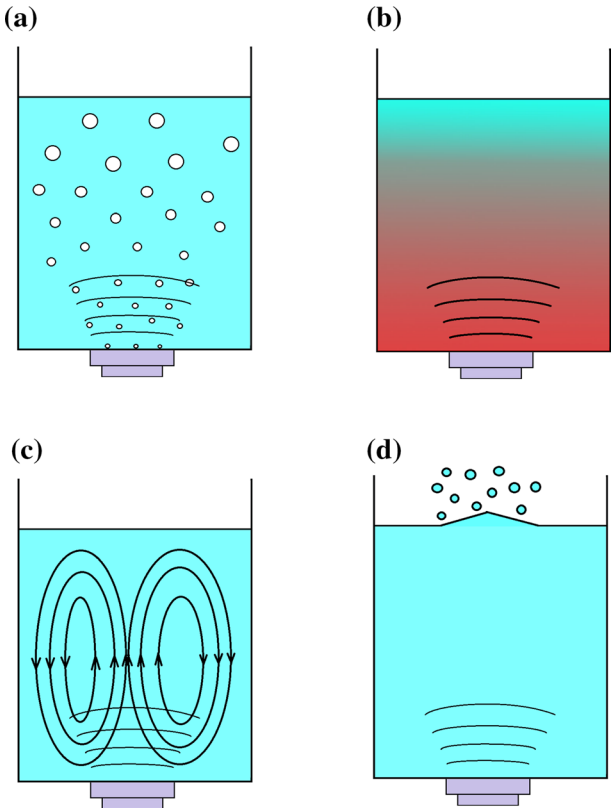

Fig. 4 Effects of ultrasonic sound propagation in liquid (a) acoustic cavitation; (b) acoustic heating; (c) acoustic streaming; (d) acoustic fountain

weakening of bonding forces, especially at solid–liquid interface. According to Oh et al. [98], ultrasonic waves can enhance the melting rate by 2.5 times compared to the case without ultrasonic vibration. However, a similar influence on the solidification rate cannot be outrightly stated as the solidification process is predominantly governed by conduction.

Vadasz et al. [99] have reported that the solidification rate could be enhanced throughout the process using vibration (frequency ranging from 10 Hz to 300 Hz). However, the enhancement rate decreases as the solidification progresses due to lack of liquid quantity as time goes. Although the authors applied only mechanical vibrations, it can be stated that vibrations (mechanical/ultrasonic) can influence the solidification process for a substantial period, if not throughout.

The ultrasonic waves are found to be very effective in enhancing the two major phases of solidification; nucleation rate (nuclei formation) and crystallization rate (nuclei's growth into a crystal) [100]. In fact, the effectiveness of ultrasonic waves in enhancing food freezing rate is extensively reported in the literature [101, 102]. When it comes to PCMs of LHTESS, no work could be found except the one by Wei and Ohsasa [103], in which only the influence of ultrasonic waves on nucleation rate is reported. Similarly, Hu et al. [104] have reported the early onset of nucleation in deionized water and sucrose solution when ultrasonic waves were used. It is clear from the above discussion that ultrasonic waves have a greater influence in advancing nucleation, which considerably reduces the overall solidification time.

Although it is proved that the crystallization rate of food products is considerably higher due to ultrasonic waves, no such conclusion can be drawn regarding PCMs of LHTESS due to the lack of reported studies. This demands a higher volume of research work to understand the role of ultrasonic waves in accelerating the solidification rate. Specifically, the progress of the second phase (after the nucleation) under the influence of ultrasonic waves should be of interest.

4.2 Optimization of Ultrasonic Power Consumption

To effect ultrasonic vibration, ultrasonic waves should be generated, and the waves should be made propagating through the fluid. The various arrangements of execution of ultrasonic vibration for phase change heat transfer are shown in Fig. 5. Ultrasonic waves can be of either low intensity (< 1 W) or high intensity (> 10 W) [105, 106]. Power ultrasonic waves are more suitable for heat transfer enhancement as they can alter the behavior of the medium through which they propagate.

The reported studies focusing on PCMs' heat transfer enhancement have employed ultrasonic waves in the range of 60–300 W power. These investigations are generally carried out on laboratory-scale setups with a small quantity of PCM. In the case of practical applications, the size of the system and thus the quantity of PCM would be obviously on the higher side. Accordingly, the number of ultrasonic transducers should be increased, which would result in higher power consumption. Hence, the ultrasonication processing should be optimized for a maximum enhancement in phase change rate with the lowest possible power input.

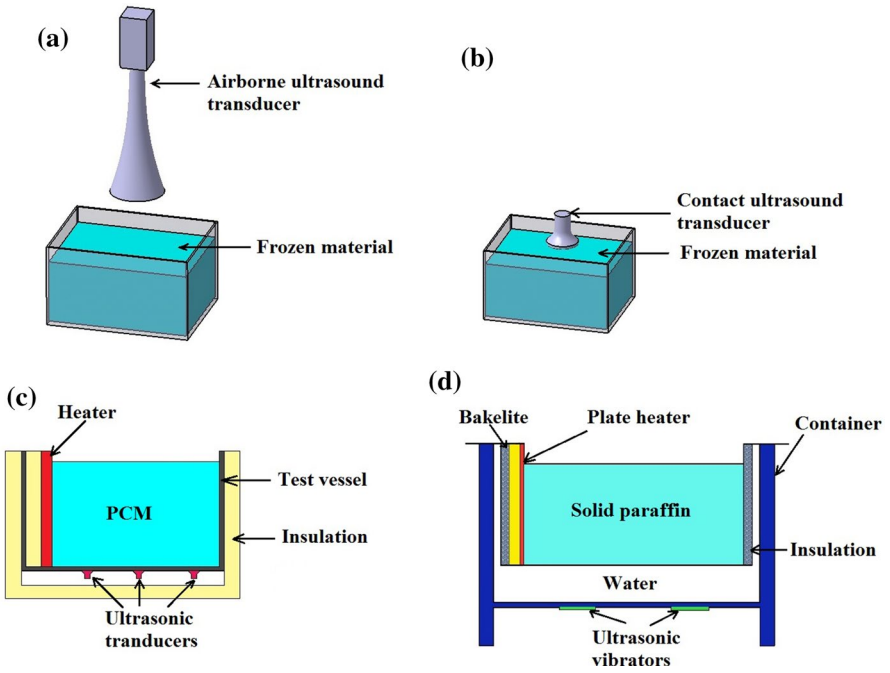

Fig. 5 Arrangements of execution of ultrasonic vibration in LHTESS (a) non-contact air borne transducer [97]; (b) device away from material [97]; (c) transducers attached to the container [98]; (d) vibrators and container wall separated by water [106]

Varying power input is relatively easier to handle as compared to frequency variation, which is evident from many papers [98, 107–109]. Although high power ultrasonic waves result in a higher melting rate, they may not always be executable due to high electricity costs. In this perspective, only the paper published by Zhang and Du [110] provides useful insights. The authors attempted to optimize the ultrasonic effect by investigating the roles of ultrasonic power, activation time, and activation duration in heat transfer enhancement. It is observed that the enhancement is significant and consistent with an increase in power. Similarly, the longer the activation duration higher is the melting rate. As already mentioned, ultrasonic waves do not have a similar impact all the time during melting. In line with this, the authors have found that activating ultrasonic waves after few minutes of melting leads to faster melting. Similarly, keeping the ultrasonication in the middle stage causes better melting than the one observed towards the end. Hence, the intermittent operation of ultrasonication seems to be a better mode to achieve the highest possible melting rate with the lowest possible power consumption. However, the exact time at which the ultrasonic waves should be activated and the activation period may vary from case to case. This may depend on the type and thermo-physical properties of PCM, its quantity, ultrasonic power input, and so on. Hence, studies may be carried out on the proposed storage system before employing the system for practical applications. Nevertheless, the reported works on ultrasound-assisted phase change processes

have demonstrated the potential of ultrasonic waves in enhancing the rate of phase change processes. Table 2 presents the list of investigations that have reported ultrasonic vibration's influence on phase-change processes.

4.3 Limitations

Although ultrasonic vibration seems to be an attractive alternative heat transfer enhancement technique for LHTESS, a couple of disadvantages are inevitable. Firstly, ultrasonic waves can be generated only by electricity. In particular, power ultrasonic waves, which are required for LHTESS, consume a high amount of electricity. This would make the system uneconomical. In addition, the storage module should be provided with additional devices such as ultrasonic transducers, facilities to attach transducers and electric power components.

5 Electrohydrodynamics Technique

Besides ultrasonic waves, an electric field can also be utilized to enhance the performance of thermal fluids. By applying an electric field, electrohydrodynamically induced fluid motion can be obtained. The electrohydrodynamically induced fluid motion is the result of various electro body forces on the fluid. These include Coulomb force, dielectrophoretic force and electrostrictive force. The details of the electro body forces can be found in Ref. [111]. Unlike the ultrasonic vibration technique, the electrohydrodynamics (EHD) technique requires less energy input. Further, this technique offers attractive advantages like fast response, absence of moving parts and quietness [112]. The EHD technique is a proven technique for enhancing the heat transfer performance of systems using single-phase fluids [113, 114]. Besides single-phase systems, it is also found to be effective for multiphase systems involving liquid–gas phase change [115–117].

5.1 EHD for LHTESS

In recent years, the EHD technique has gained considerable attention in PCM research. The enhancement of the melting rate is of particular interest. As already mentioned, the heat transfer enhancement by the EHD technique is due to the electro body forces. Hence, it is important to understand the role of these body forces along with the buoyancy forces that exist within the liquid PCM.

In the pioneer study, Dellorusso [118] observed that the tested geometry of the storage module could not enhance the natural convection and hence, not much enhancement in melting rate under the application of EHD. This outcome indicates that if natural convection due to the buoyancy force is not enhanced, then the impact of EHD would be insignificant. Hence, Nakhla et al. [111] employed a geometry wherein the melting heat transfer was governed mainly by conduction. The aim was to investigate the role of EHD in enhancing the melting rate in the absence of natural convection. Accordingly, a rectangular module of $126 \times 36 \times 50.8$ mm was fabricated

Table 2 Investigations on ultrasonic vibration assisted phase change process

References	System & PCM used	Vibrator specifications	Mechanism	Nature of work & phase change process	Major outcomes
Fairbanks [96]	Beaker & frozen coal in water	Frequency 20 kHz	Airborne ultrasound applied without contacting the PCM Ultrasound applied by having direct contact with PCM	Experimental & melting	Direct contact ultrasound results in higher melting rate Non-contact method is ineffective even when compared to conventional heating
Choi and Hong [97]	Rectangular vessel & n-octadecane	15–55 kHz frequency and 60 W power	Bottom of the container provided with 3 Piezo electric transducers of 3.5 cm diameter which vibrate the wall at ultrasonic frequency	Experimental & melting	Melting time decreases with the increase in ultrasonic frequency All the ultrasonic effects contribute to heat transfer enhancement
Oh et al. [107]	Square cavity & n-octadecane	40 kHz frequency and 70–340 W power	Vibrators are not placed directly on the bottom of the cavity rather placed on another bottom plate which is separated from cavity by water	Experimental & melting	Melting rate increases by 2.5 times due to ultrasonic vibration Solid PCM is also influenced by ultrasonic waves
Oh et al. [108]	Rectangular cavity & n-octadecane	28 kHz frequency and 161.9 Wh power	Vibrators are not placed directly on the bottom of the cavity rather placed on another bottom plate which is separated from cavity by water	Experimental and numerical & melting	Acoustic streaming is the prime factor for enhancing the heat transfer rate Acoustic streams develop thermal osculating flow

Table 2 (continued)

References	System & PCM used	Vibrator specifications	Mechanism	Nature of work & phase change process	Major outcomes
Zhang and Du [110]	Cylindrical stainless-steel unit & palmitic acid-stearic acid eutectic mixture	40 kHz frequency 40–150 W power	The cylindrical container is placed in a water bath which is subjected to ultrasonic vibration	Experimental	Higher melting rate is observed with higher power Longer the activation duration higher is the melting rate
Yang and Oh [109]	Rectangular enclosure & n- octadecane	40 kHz frequency 230.5 Wh power	Vibrators are not placed directly on the bottom of the cavity rather placed on another bottom plate which is separated from cavity by water	Experimental and numerical	Ultrasonic vibrations result in lower final temperature of PCM in comparison with conventional case Lower energy consumption with ultrasonic assisted melting as compared to conventional melting
Wei and Ohsasa [103]	Glass beaker & Sodium acetate trihydrate (SAT) and erythritol	38 kHz frequency	The beaker is placed in a water bath which is subjected to ultrasonic vibration	Experimental & solidification	Inducement of nucleation is delayed if ultrasonic vibration alone is employed Combination of ultrasonic waves and nucleation agents results in enhancement of nucleation rate

to store paraffin wax. The PCM was heated from the top, and the high voltage electric field (−8 kV DC) was applied using horizontally arranged 9 electrodes. A significant enhancement in melting rate is reported as the melting time was reduced by 40.5 % compared to the case without EHD. In order to observe the enhancement mechanism, digital images were captured using a high-speed camera. The images have revealed an interesting phenomenon, termed solid extraction, which refers to the extraction of solid dendrites due to the EHD body forces from the mushy zone towards the melted region. This could induce convection in the liquid PCM, and thus high melting rate was achieved. Hence, it is concluded that EHD body forces are applied on the interface of solid and liquid and molten PCM. The role of each force is further investigated in the subsequent work [119].

The test unit was similar to that of the previous work, but two heat exchangers were used at the top and bottom of the storage unit. The top one carried hot water, whereas cold water was allowed to flow through the bottom heat exchanger. This was to make sure that no natural convection existed. The electric field was applied through 23 electrodes arranged in three rows. It is reported that only Coulomb forces have a greater influence on solid dendrites as they force the charged dendrites to move towards the mushy region. The impact of dielectrophoretic forces is found to be minimum. Hence, Coulomb forces are the major reasons for the electro-convection in the liquid PCM. It is clear from the above-discussed works that the EHD technique enhances the conduction dominated melting process. However, in practical systems, natural convection in the liquid PCM generally dominates the melting. Hence, it is important to explore the impact of EHD on the natural convection dominated melting process.

In view of this, Nakhla et al. [120] employed a vertical configuration in which the PCM was heated from the side. Even with electrodes (30 Nos), the existence of natural convection in this module is demonstrated as the heat transfer coefficient was found to be higher at the bottom of the unit than that at the top portion. When the electric field was applied, a different form of convection cells could be observed. Due to EHD, the larger natural convection cells that existed initially were divided into multiple cells in the gap between the electrode rows. The multiple cells are nothing but the combination of electro and natural convection cells. This indicates that electro-induced convection could interact with the natural convection, and the net convection effect becomes stronger.

It is obvious that natural convection exists even in the horizontal oriented system if the PCM is heated from the bottom. To study the effect of EHD in such an arrangement, Selvakumar et al. [121] considered a rectangular cavity in which the PCM was heated from the bottom plate. The bottom plate also acted as electrodes. The numerical results have shown different stages of convection dominated melting. Although Coulomb forces existed throughout the melting process, the onset of electro-convection was observed only after the presence of a certain quantity of liquid PCM. Nevertheless, significant enhancement due to EHD is reported. In fact, the viscous effect in the liquid PCM could be overcome by the Coulomb force shortly after the onset of electro-convection. Similar results are also presented by Luo et al. [122]. Hence, it can be stated that the EHD technique has a positive impact on natural convection dominated melting also.

5.2 Generation of Electric Field

To induce EHD forces, a strong electric field is critical, which can be generated by applying high voltage. As mentioned already, wire electrodes were employed in the works reported in the Refs. [111, 119, 120]. Although these electrodes are of smaller diameter (around 3 mm), significant numbers were employed. Moreover, they ran through the system across (Fig. 6a). Hence, there would be a reduction in PCM volume.

In the recent work, Sun et al. [123] have proposed using walls of the heat exchanger as electrodes. Two heat exchangers, one for carrying hot HTF and another for cold fluid, were positioned on either side of the vertically oriented rectangular storage unit. In the experiments, either hot or cold heat exchanger was applied with an electric field, and the other was grounded (Fig. 6b). The relative performance of hot and cold electrodes will be discussed later. In any case, the electrodes were a part of the storage unit, and hence, the PCM volume was not affected due to the absence of electrodes in the PCM.

Although the tested unit by Sun et al. [123] was a laboratory-scale model, the concept of utilizing heat exchanger surface as electrodes can be extended to real-time systems. For example, in shell and tube configuration, which is widely used in solar thermal and heat recovery applications, the HTF flows through the central tube and PCM is loaded in the shell around the tube. During melting, the tube wall remains hot, whereas the cold one is nothing but the wall of the shell. Hence, without adding additional structure in the PCM, the wall of the tube or shell can be used as an electrode (Fig. 6c).

While applying an electric field, the polarity of the electric voltage may be one of the concerns. In fact, both positive and negative voltages are tried and found to enhance the melting performance [111, 119, 120]. However, the relative strength

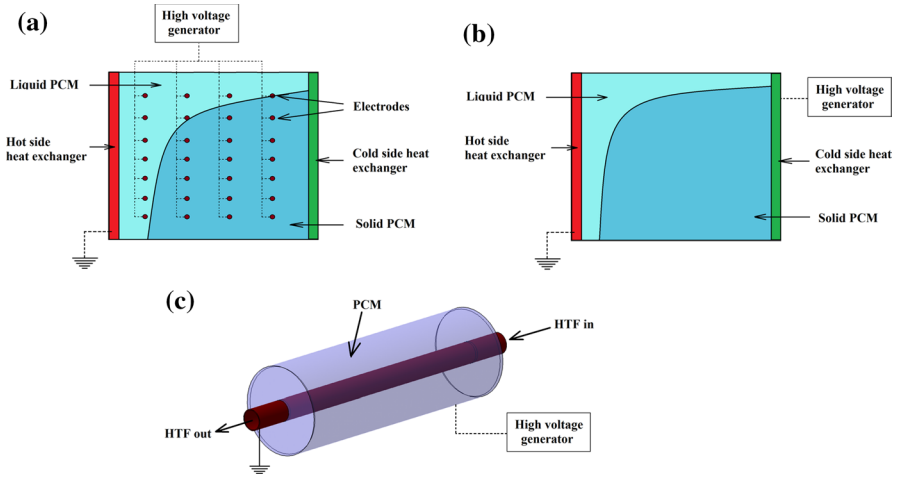

Fig. 6 Electrodes in EHD technique (a) wire electrodes [111, 119, 120]; (b) cold heat exchanger as electrode [123]; (c) wall of shell as electrode

is not discussed in these works. Sun et al. [123] applied both positive and negative voltages on the same test facility and reported negligible differences. Hence, the voltage can be either positive or negative as applicable. However, Sun et al. [123] have significant differences between hot and cold electrodes irrespective of the polarity of the applied voltage. In the case of a hot electrode, the EHD technique could not enhance the melting; rather, it has a negative effect. This is due to the attraction of liquid PCM towards hot electrodes, which effectively prevents the flow of liquid along the interface. Therefore, natural convection is hampered. Further, the increase in voltage on the hot electrode resulted in a reduced liquid fraction. On the other hand, cold wall as an electrode is proven to be effective as enhancement in melting rate was observed, and enhancement was consistent with an increase in applied voltage.

Besides polarity, the role of applied voltage form, i.e., AC or DC, is also explored in the literature. Among the reported works, Nakhla et al. [119] provides better information on the distinction between AC and DC power. The system with AC power could not yield any enhancement, whereas the DC power system exhibited significant enhancement in melting rate. Between the two phases of DC power, there is a difference in electric permittivity. The dielectrophoretic force is caused by electric permittivity. As already discussed, the dielectrophoretic force is insignificant in enhancing the melting rate. Hence, AC power could not make any impact on melting.

5.3 Limitations

Although the EHD technique seems to be the simplest, at least in comparison with the ultrasonic vibration technique, a couple of disadvantages pose challenges as far as practical application is concerned. Considering the past research, the technique applies mainly to the melting process, and the effect on solidification is unknown. Secondly, the EHD technique can be employed only if the PCM is dielectric like paraffin wax. In the case of salt hydrates, which are electrically conductive, they get affected by the strong electric field. Further, PCMS with high electric conductivity will consume a high amount of energy. To the best of the authors' knowledge, all the reported works have employed only PCMs, which are dielectric.

6 Displacement of PCM

An exciting and promising technique for improving phase change heat transfer rate is keeping the PCM moving during phase change with the help of some external aid. Since PCM keeps moving, the heat transfer is majorly governed by forced convection, and thus the thermal resistance is considerably reduced [124]. Further, the phase segregation problem which generally exists with the conventional system can be alleviated with moving PCM. Literature reveals a few approaches in connection with the continuous movement of PCM.

(1) SHX
(2) Recirculation of liquid PCM
(3) PCMflux concept
(4) Scraping of solidified layer

   (i) Moving scrapers
   (ii) Fixed scrapers or rotating drum

Although only limited investigators employ the listed techniques, adequate information can still be explored.

6.1 SHX as LHTESS

The SHX finds its application in many industrial processes wherein transportation and heating/cooling take place simultaneously [125–131]. Invariably, those processes involve solid materials, and only sensible heat transfer takes place. On the other hand, SHX is also involved in phase change heat transfer as they are well-known in polymer melting (extrusion) [132–135]. In the case of LHTESS, the employment of SHX is proposed by the research group at Fraunhofer ISE, Germany [136]. The proof of concept, the performance, benefits, and challenges/issues are extensively discussed through a series of papers [136–139]. The studies focusing on the application of SHX for various purposes are summarized in Table 3.

6.1.1 The System Components and Issues

An SHX should have one or more rotating shafts with screw threads on the periphery. The material to be transported is fed on the surface of the screws so that it can move forward as the shafts rotate. For processing, for instance, polymer extrusion, the inner surface of the casing does have heating elements. In LHTESS, there is an HTF that demands flow paths. As the PCM moves along the periphery of the shafts, the HTF can be made flowing through the shafts which are hollow. Accordingly, the SHX developed at Fraunhofer ISE uses not only the hollow shafts but also the hollow structured screw flights and the troughs for HTF circulation [139]. The cross-section of the typical double screw heat exchanger employed for LHTESS is shown in Fig. 7.

To facilitate PCM transport during charging and discharging, the system is provided with an additional conveyor (to transport solid PCM) and pump (to transport liquid PCM). Additionally, a crusher is used to maintain the size of the solid PCM granules uniform, which comes out of the SHX after discharging. Figure 8 illustrates the general arrangement for PCM transport. Uniform sized granules are critical in maintaining the uniform mass flow rate of PCM at the inlet. Overall, the screw shafts, along with additional components mentioned above, seem to increase the system complication. Moreover, the increase in the number of power consumption devices might counter the benefit of enhanced heat transfer. Zipf et al. [136] have reported that the power consumption could be less than 3 % of the total energy

Table 3 Application of SHX in various fields

References	Medium	Description of SHX	Nature of work	Highlights
Waje et al. [127]	Fine crystalline solid	Jacketed conveyer, air swept by nitrogen Heating medium: hot water	Experimental	92 % moisture removal rate is obtained with a thermal efficiency range of 25 % to 62 %
Kaplan and Celik [129]	Woodchips	Co-current and counter-current arrangement for drying woodchips of 0–2 mm and 2–5 mm size Drying agent: Hot air at 20 $m^3 \cdot h^{-1}$ Screw rotation speed: 10 rpm	Experimental	Moisture content is reduced by 12 % using co-current arrangement
Cucumo et al. [130]	Sand	Screw angle of 20 °C, with indirect heat exchange Heating medium: hot water at 80 °C	Experimental and numerical	Moisture reduction of 30 % is observed Different sources of heat could be used for drying of constructional aggregates
Chung [133]	Polymer	Single-screw extruder	–	Highlighted the extrusion operation, desirable polymer properties and environment conditions
Ershov and Trufanova [134]	Polymer	Three channel geometries (flat and cylindrical model with and without gap) were analyzed	Numerical	Flow and heat transfer studies are performed in the extruder screw channel, output adapter and forming tool of the SHX Polymers' viscosity dependence on shear rate and temperature is studied
He et al. [135]	Polymer	Single-screw extrusion Sub-macroscopic visual system, thermographs and instruments are used to visualize the melting of granule	Experimental	Melting proceeds from outside towards inside Granule melting and bulk melting occur simultaneously
Zipf et at. [136]	Eutectic mixture of $NaNO_3$ and KNO_3	Laboratory prototype of SHX with an eutectic mixture of $NaNO_3$ and KNO_3 is used as PCM	Experimental	The dependency of PCM mass flow, rotational speed of the screw shaft, temperature difference between PCM and HTF, heat exchanger inclination and granular size on heat transfer characteristics is analyzed

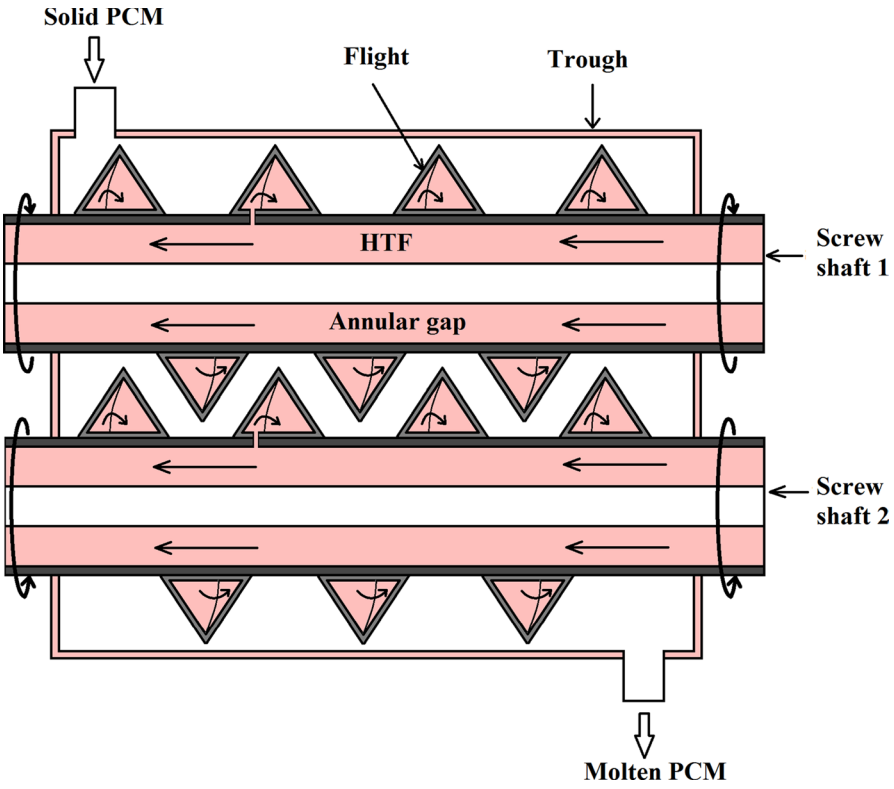

Fig. 7 Sectional view of a typical double screw heat exchanger for LHTESS [138]

stored/retrieved. However, extensive experiments with a real scale model are to be carried out to draw a firm conclusion on the storage efficiency of the SHX, taking into account the power consumption by additional devices.

6.1.2 Storage and Transport of PCM

Unlike conventional storage systems, SHXs do not offer any storage space within. Hence, separate storage tanks need to be accommodated in the loop. Although two separate tanks, one each for solid and liquid PCMs are sufficient, Zipf et al. [137] have recommended an additional tank for superheated PCM in solar thermal power plants to achieve high-temperature steam discharged to the turbine. Otherwise, the system temperature would have been less due to the indifferent thermo-physical properties of HTF (steam) and PCM ($NaNO_3$). In any case, a higher HTF temperature at the outlet during discharging is beneficial. At the same time, there must be a trade-off between system complication/initial cost and storage efficiency, which needs further study with different combinations of PCM/ HTF.

Zipf et al. [136] implemented two different mechanisms for solid PCM tank and liquid PCM tank to accomplish the PCM transport between the tanks and heat

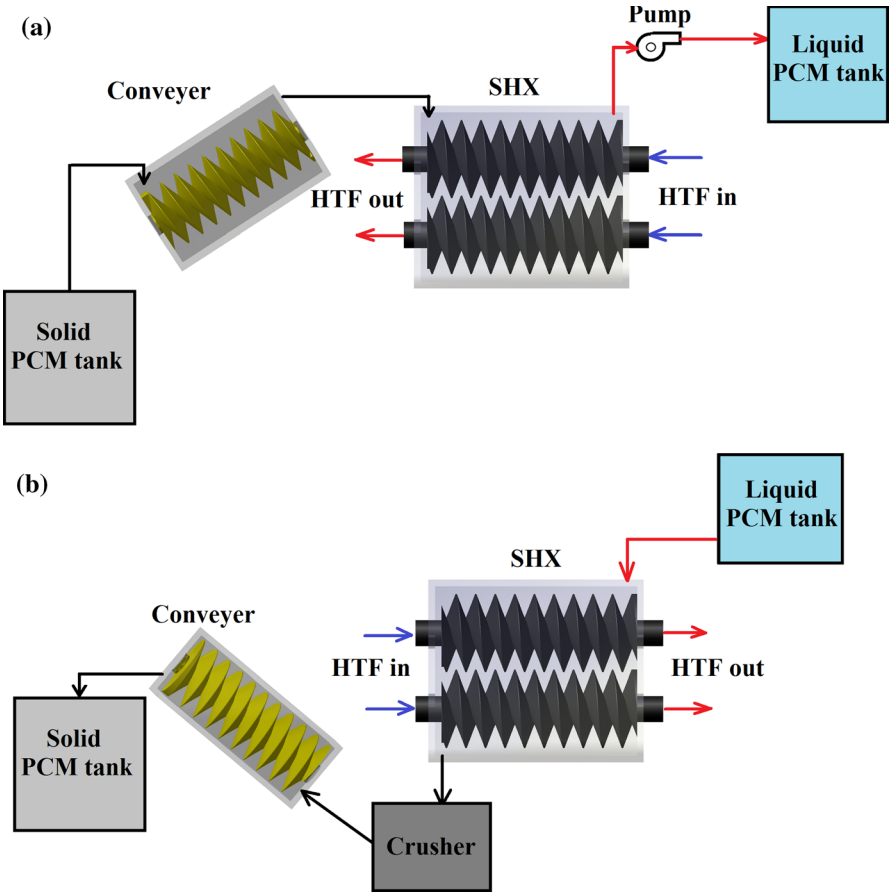

Fig. 8 Arrangements of PCM transport to and from SHX [137] (a) charging; (b) discharging

exchangers during cyclic operation. For solid PCM, three conveyors were employed, and the operation of those depends on whether the storage supplies or receives PCM. As mentioned earlier, a crusher also comes into operation during discharging to control the size of the PCM granules stored in the tank. On the other hand, the liquid PCM tank was provided with a crane mechanism that can change the location of the tank between the inlet and the outlet of the SHX. It should be mentioned that the set-up requires an automated operation to a certain extent.

Besides the transport of PCM between tank and SHX, it is important to address the issues connected to PCM's transport within SHX. In principle, once the PCM is supplied through an inlet, the rotation of the screw shafts would carry it up to the outlet through which the PCM in the changed phase can be delivered to the corresponding tank. The PCM should be distributed uniformly for maximum utilization of the available heat transfer area. The SHX developed at Fraunhofer ISE consists of two co-rotating screw shafts. The two shafts are made rotating at different speeds

by providing a single thread on one shaft and two threads on the other. This arrangement seems to have a positive impact on self-cleaning. The rotation of the screw shafts causes the PCM, which is supplied in the middle, to move in a radial direction in addition to axial direction transport. This leads to forming a thin layer of solid PCM on the right wall throughout, which results in the underutilization of the heat transfer area. To overcome this, it is proposed to supply the solid PCM along the left side of the screw shaft. Even with such an arrangement, Zipf et al. [136] could not achieve uniform distribution of solid PCM. Further, the melting of solid PCM was not complete at higher speeds. On the other hand, lowering the speed affected the PCM flow rate. A dam kind of arrangement is recommended to overcome the above issues. However, the effectiveness of such an arrangement is yet to be investigated.

For the distribution of liquid PCM, Zipf et al. [136] employed five control valves that could cover only 30 % of the total available heat transfer area. Hence, it was redesigned, which used a wall to distribute liquid PCM [139]. To avoid solidification while distributing through smaller holes, a trace heating arrangement was employed. With this, the system could achieve around 70 % coverage of the heat transfer area. In one of the subsequent works, Zipf et al. [138] have recommended spraying liquid PCM on the shafts to enhance the distribution. Although it is not yet experimentally verified, it seems to be an effective and less complicated one.

6.1.3 Heat Transfer Performance

The existence of forced convection due to the flow of PCM in SHX makes it superior to conventional types as far as heat transfer performance is concerned. Unlike natural convection, the forced convection can be maintained consistently by controlling the operational parameters like shaft speed, flow rate, etc. Hence, the phase change rate in SHX would be near-constant during melting and solidification. However, the solid PCM layer still poses a challenge as the heat transfer coefficient during discharging was observed to be less in comparison with the charging process [138]. In order to overcome this, the clearance between the connecting screw flights and the flights and troughs should be as small as possible. The authors have reported that the clearance and thus the thickness are determined by the geometry, material and manufacturing process involved. However, the effects of these factors on the thickness of the solid PCM layer are yet to be studied. In conventional storage systems, the entire area is available all the time during the phase change processes. As discussed earlier, this is a bottleneck in SHXs, which may downgrade the benefits expected due to forced convection.

6.1.4 Limitations

LHTESS, which employ the SHX technique, generally comprises multiple components, including separate PCM tanks, conveyors to transport PCM between tanks and SHX, and crusher. Hence, the system is highly complicated and bulky. Specifically, the employment of SHX technique for LHTESS results in the most complicated system among the various alternative heat transfer enhancement techniques. Further, additional pumping power is required for PCM transport.

6.2 Recirculation of Liquid PCM

If the melted layer near the heat transfer surface is taken out, then a new solid layer would come in close to the heat transfer surface, and further melting would occur. If it continues, the melting process would be dynamic. The dynamic melting would result in a higher melting rate compared to the conventional case wherein only static melting is possible. It should be noted that the liquid layers taken out have to be brought back to the system. This means that the liquid PCM is recirculated. This technique of displacing PCM seems to be much simpler than the SHX concept.

6.2.1 Arrangement for Dynamic Melting

In the pioneer study by Tay et al. [140], Copper tubes inserted in the tank were used to carry HTF. For dynamic melting to occur, an additional tube (U-shaped) was employed with several small holes drilled (Fig. 9a). However, the U-tube did not carry HTF; instead, it held a small tube that carried HTF. Since this smaller tube ran through the U-tube, it had direct contact with PCM at the base of the U-tube through

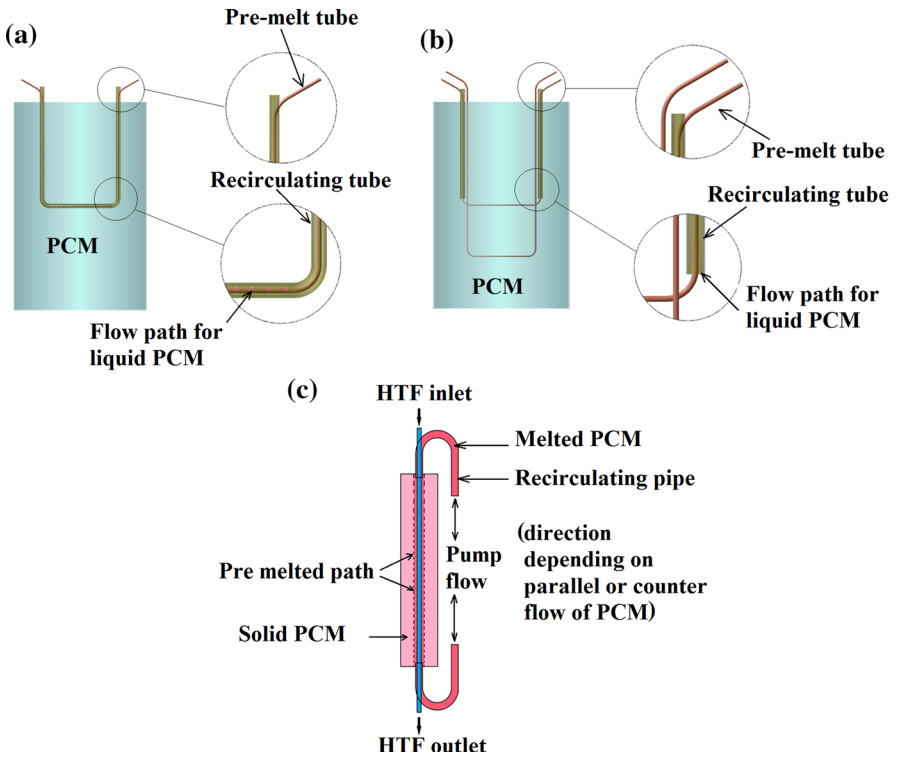

Fig. 9 Various arrangements employed for establishing pre-melt recirculation (a) U-tube with pre-melt tube [143]; (b) two U-tubes and pre-melt tubes [143]; (c) tube attached to shell side of shell and tube module [144]

the smaller holes. Hence, the smaller holes provided the flow path for the melted PCM. Since the U-tube was connected to a pump, the recirculation of liquid PCM was ensured. Although this arrangement exhibited promising results in terms of heat transfer enhancement, the investigators observed inconstancy in the results.

Intending to improve the effectiveness, the same authors [141] employed a different design in the subsequent work. The improved design used two smaller HTF tubes; both form U-shape (Fig. 9b). The vertical sides of one of the tubes were covered by other bigger-sized tubes connected to the pump. The horizontal part, located at the center of the tank, was in direct contact with PCM. Hence, the PCM around the horizontal part and the uncovered portions of vertical sides would flow through the vertical tubes connected to the circulating pump. The second U-tube was fully exposed as none of the portions was covered. It was placed so that the horizontal part was positioned at the lower portion of the tank, and the vertical sides were positioned close to the vertical sides of the first U-tube. This arrangement aimed to create a flow path for the PCM at the lower portion of the tank. This design was found to be producing better heat transfer enhancement as the melting time was shorter than that of a conventional system.

Tay et al. [142] have numerically studied the effectiveness of dynamic melting in shell and tube heat exchanger. The vertically oriented module allows the HTF to flow downward through the central tube, and the annular space between the tube and shell holds the PCM. Once a sufficient amount of liquid PCM is established around the tube, the same can be taken out either from the top or the bottom using a pump and supplied back to the system at the opposite end (Fig. 8c). Depending on the end from where the liquid PCM is taken out, the flow is either parallel or counter with the HTF flow. In parallel flow, the recirculation was realized by admitting the liquid PCM at the top end. Since the HTF also entered from the same end, the temperature difference between HTF and PCM was higher at the top portion as compared to remaining portions. This obviously resulted in a higher liquid fraction at the top and a gradual increase in solid fraction downwards. This indicates that the parallel flow recirculation tends to assist the portion of PCM where the melting rate is already higher. However, the PCM at the lower portion melts at the same rate due to the lack of dynamic melting. On the other hand, the counter flow arrangement works in another way as it promotes dynamic melting and enhances the melting rate where it is most needed. According to the results of Tay et al. [142], the counter flow arrangement was more effective than parallel flow only when the PCM flow rate was moderate. Moreover, Gasia et al. [124] have observed that the drop in liquid PCM level during melting caused cavitation problems in the pump.

6.2.2 PCM Recirculation

Since the pump is designed for liquid PCM, it is important to ensure that no solid PCM is admitted into the pump. Tay et al. [140] have observed that the solid PCM entering into the pump caused choking. As a result, the speed of the pump started decreasing. Hence, the pump should be operated only after the PCM close to the heat transfer surface is fully melted. According to Tay et al. [141], the pump can be switched on once the PCM temperature is sufficiently higher than the melting

point. However, switching on the pump at a temperature much higher than the melting point, may nullify the effect of dynamic melting. Gasia et al. [124] have reported that the threshold value for water (PCM) is 5 ± 0.5 °C.

Besides the timing of pump operation, the flow rate of PCM should be appropriate as it has a significant role in making dynamic melting effective. It is expected that the enhancement in heat transfer rate would be consistent with the increase in PCM flow rate. However, Tay et al. [142] have reported that the enhancement is significant if the flow rate of PCM is higher than that of HTF. If there is no recirculation, the melted PCM that remains inside throughout the process helps melt the solid PCM. It is evident that the recirculation of PCM affects the presence of melted PCM and the heat transfer area available for solid PCM. Hence, the mixing rate, which is determined by the flow rate of PCM, should be sufficient enough so that the loss in the heat transfer area is overcome.

The circulated PCM tends to gain additional heat associated with pumping. Secondly, it may absorb heat from outside while flowing through an external pipe. Since the hotter PCM moves along the tube wall continuously, the outlet temperature of HTF would be higher than that is observed in a conventional case. This reduces the difference between inlet and outlet temperatures of HTF and thus the heat transfer effectiveness. The results of Gasia et al. [124] have revealed that the reduction in effectiveness is found only at PCM flow rates lower than the HTF flow rate. When the flow rate of PCM is higher than that of HTF, the degree of mixing is sufficient to overcome the impact of heat gain. Further, the results obtained from the pumping power analysis have shown that it works the other way round. Hence, it is concluded that the cost involved in connection with the pumping system is negligible.

6.2.3 Heat Transfer Enhancement

The extent to which heat transfer rate is enhanced by dynamic melting is revealed by Tay et al. [140]. It is observed that the heat transfer rate could be increased two-fold by dynamic melting. This is attributed to the fact that the effective thermal conductivity was doubled by dynamic melting. Because of the higher heat transfer rate, the average effectiveness was found to be significantly high. Further, the melting process took less time to complete. Hence, it can be stated that dynamic melting improves the thermal performance of LHTESS in all aspects. Besides improving the effectiveness, dynamic melting does not allow the local effectiveness to drop throughout melting [142]. In a conventional system, the temperature difference between HTF inlet and outlet decreases as melting progress, whereas the temperature difference between HTF inlet and the melting point of PCM remains constant. Hence, the effectiveness, which is the ratio of the above two temperature differences, tends to decrease during melting. However, the mixing of liquid PCM leads to a drop in PCM temperature in dynamic melting. This results in a sudden drop of HTF temperature and an increase in temperature difference between HTF inlet and outlet [124]. Hence, improvement in the effectiveness of the system can be realized.

As mentioned earlier, the enhancement by dynamic melting is well pronounced once the mass flow rate of PCM is higher than that of HTF. This is further demonstrated in the recent study by Gasia et al. [143], in which higher PCM velocities

resulted in a higher heat transfer rate. Consequently, the melting time was found to be shorter as the PCM velocity increased. If the liquid PCM is pumped at a higher velocity, the difference between the temperatures of the inlet and outlet of the circulation line would be negligible. This allows the liquid PCM to enter into the system at low temperature and the temperature difference between HTF and PCM remains higher, which improves heat transfer rate. As already mentioned, Tay et al. [142] have reported that PCM's mass flow rate (or velocity) should be higher than that of HTF. This sets a threshold value for PCM velocity below which heat transfer rate enhancement could not be achieved. However, the results of Gasia et al. [143] have revealed that the heat transfer rate is influenced purely by PCM velocity, and its relative value with HTF velocity has no influence.

6.2.4 Limitations

The foremost issue with dynamic melting is the commencement of recirculation. Although Gasia et al. [124] have recommended some threshold values with reference to PCM temperature, the same may not apply to all PCMs/systems. Hence, it is important to identify the temperature of PCM at which the pump can be started. Further, starting and shutting off of the pump should be automated based on the temperature of the PCM during melting. Even though the cost of the pump operation may not be significant, the pump along with the recirculation line increases the complexity of the system. Because of the recirculation line, there may be a PCM leakage problem, which should be addressed while designing the system. Moreover, the heat gain in the recirculation line demands adequate insulation.

Besides the above issues, there is a limitation that does not have a solution. As the name implies, it can be employed to improve the thermal performance only during melting. In most cases, performance enhancement is needed for both melting and solidification. In fact, solidification should be given preference as it takes place at a slower rate than melting. In such a scenario, an additional technique should be executed for solidification along with dynamic melting.

Despite the issues mentioned above, the results of the reported research seem to be promising. However, considering the limited quantity of reported research so far, further research is suggested. Table 4 presents the outcomes of studies on the PCM recirculation technique.

6.2.5 PCMflux Concept

Moving PCM techniques also help in avoiding the drop in heat flux during the phase change process. Especially during the discharging (solidification) process, the growing solidified PCM layer on the heat transfer surface results in a consistent drop in heat flux. If the PCM is continuously moved during the process, the above issue can be overcome and hence, a nearly constant heat flux can be maintained. With this in mind, another technique is developed with movable PCM called the PCMflux concept [144].

Table 4 Studies on PCM recirculation technique

Reference	Description of the study	PCM	Nature of work	Highlights
Gasia et al. [124]	Shell and tube arrangement with recirculation of melted PCM with flow rates of 0, 0.5, 1 and 2 LPM	Water	Experimental	66 % increase in heat transfer rate, 65.3 % reduction in melting time and 56.4 % increase in effectiveness are observed at the PCM flow rate of 2 LPM
Tay et al. [140]	Tube-in-tank storage system with U-tube coil arrangement and a pre melt tube for HTF circulation were used. Melting behavior of PCM with different temperature gradients and flow rates were analyzed	Salt hydrate	Experimental	Improved storage system effectiveness with reduced melting time
Tay et al. [141]	Tube-in-tank storage system with U-tube coil arrangement and two pre melt tubes for HTF circulation were used	Salt hydrate	Experimental	Improved design shows increased effectiveness and reduced melt time as compared to single melt tube arrangement
Tay et al. [142]	Forced recirculation of melted PCM in parallel and counter flow arrangements	Sodium nitrate	Numerical	Effectiveness increases with HTF mass flow rate Phase change time is reduced by 15 % to 80 % Counter flow arrangement could be effective only when the PCM flow rate is moderate
Gasia et al. [143]	Transient behavior of LHTESS by incorporating dynamic melting technique is simulated	Water	Numerical	Parallel flow arrangement exhibits higher heat transfer rates and lower melting times as compared to counter flow arrangement

6.2.6 Basic System

In the PCMflux concept, the PCM is made moving over the heat exchanger pipe at a controlled rate. Unlike the SHX system, the PCMflux system does not allow direct contact between PCM and heat transfer surface. Instead, the PCM is carried in containers (encapsulation). The direct contact may arise material damage issues as a result of corrosion and thermo-mechanical stress (developed due to indifferent densities of liquid and solid PCMs) [145]. Since direct transport of PCM is avoided, the mechanism for PCM displacement becomes simple, less expensive and requires less maintenance. However, as the PCM is separated from the heat transfer surface, there is a dry contact with surface irregularities, which is undesirable from a friction point of view. More importantly, dry contact results in high thermal resistance due to the presence of air between the contact surfaces and hence, it is important to maintain a fluid layer between the PCM wall and heat transfer surface. The presence of a fluid layer is expected to make effective thermal contact.

6.2.7 System Details and Variants

In the pioneering work, in which the proof of concept is presented, Pointner and Steinmann [144] employed multiple thin wall containers made of Aluminium foils. The containers were connected with each other through wires, and the entire container link was moved by pulling the wires with the help of an electric motor. The containers were moved in one direction for charging and in the opposite direction for discharging.

The heat transfer zone is nothing but a bowl-shaped heat exchanger, and the pipe was arranged so that the HTF could flow in the direction perpendicular to the direction of movement of PCM containers. The fluid layer used for avoiding dry contact filled the bowl. Because of the bowl-shaped arrangement, the containers moving over the ramp could slide inside the bowl, making thermal contact with the heat exchanger pipe. Once the phase change process is over, the containers leave the heat transfer zone by rising over the bowl. The bowl-shaped heat exchanger configuration helps contain the fluid layer in the heat transfer zone and avoids the requirement of a large volume of fluid to cover the entire system. Unlike the bigger container, the smaller containers need not have stiffer walls. Besides the above, the entire bowl would act as a fin for the heat transfer pipe.

The system detailed, shown in Fig. 10, is nothing but a horizontal arrangement as the containers travel in a horizontal direction. On the other hand, a vertical arrangement is also found in the literature [146–148]. In the vertical arrangement, the PCM containers arranged as parallel layers move vertically over the finned heat transfer pipes surrounded by the fluid layer. Because of the vertical configuration, the containers can move on both sides of each pipe. This allows doubling the PCM volume for the same heat transfer rate compared to the horizontal configuration [145]. However, this arrangement has a couple of issues from a practical point of view. As multiple heat transfer zones exist, it is important to keep the distance between container and heat transfer zones as minimum as possible. With small gaps, the danger of PCM blockage increases [145]. Secondly, if the shape of the containers changes,

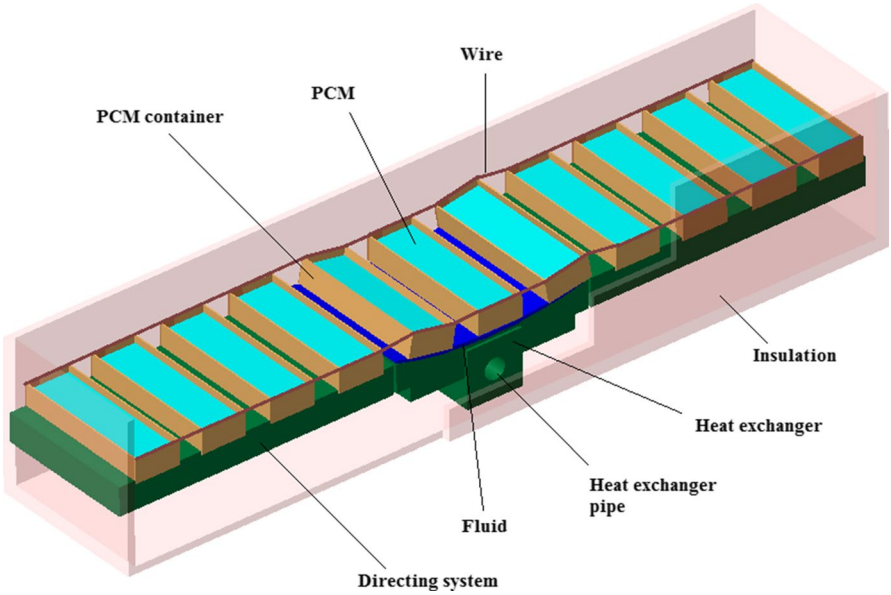

Fig. 10 Schematic of the horizontal PCMflux system [148]

they would be stuck and ultimately would result in system collapse. This demands stiff container walls, which would be uneconomical [147].

Besides horizontal and vertical arrangements, a third variant is also proposed by Steinmann [145] in which the container is a rotatable tube placed on the bowl. The rotation of the tube allows the PCM to move, and once the phase change process is over, the liquid PCM can be collected from the lower portion of the tube. Hence, the supply/collection of liquid PCM takes place on its own. Although this design seems interesting, no other details could be explored due to a lack of investigations. The three variants for PCMflux concept implementation are illustrated in Fig. 11.

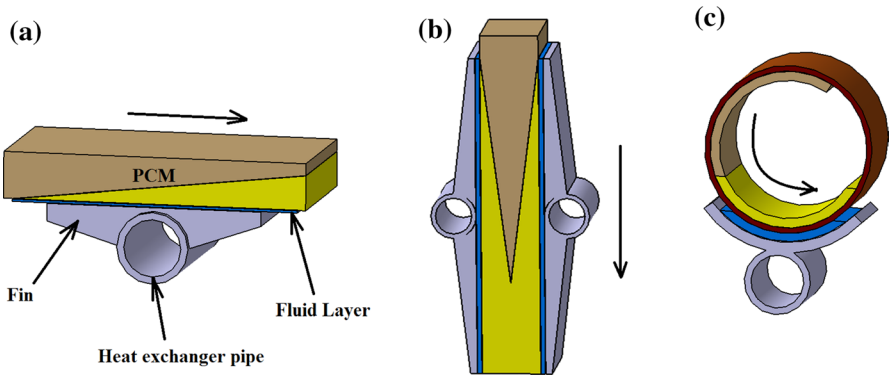

Fig. 11 Variants for PCMflux concept implementation [147] (a) horizontal; (b) vertical; (c) circular

The potential of the PCMflux concept is demonstrated only with a system having one heat-transfer pipe (one heat transfer zone). The phase change length of the PCM relies on the single heat transfer pipe, and the PCM has to move over the heat transfer zone for a distance equal to its length in the direction of movement. In this perspective, Steinmann [145] has reported the distributed module in which multiple heat transfer pipes with individual bowls and fluid layers are available. With this arrangement, the distance to be moved by the PCM is reduced by $1/n^{th}$ of the original distance (where n is the number of heat transfer zones). This permits reducing the feed rate, which is an attractive benefit. However, such a module needs further physical validation.

6.2.8 Significance of Intermediate Fluid Layer

The presence of a fluid layer that provides the wet contact, enhances the heat transfer by around 10 times compared to dry contact [147]. The employed fluid is expected to satisfy a couple of requirements. Firstly, the fluid should have higher thermal conductivity for better thermal contact. Secondly, the melting temperature of the fluid should be less than the operating temperature of the system. This is to ensure the liquid state of the fluid throughout the phase change processes so that the movement of the containers is not restricted. Although liquid metals may be suitable candidates, the cost involved works against them [145]. In the few experimental studies reported, the eutectic mixture $NaNO_2$-$NaNO_3$–KNO_3 was employed as an intermediate fluid for the PCM (another eutectic mixture, KNO_3–$NaNO_3$) [144, 147, 149]. Since the melting temperature of the eutectic mixture (fluid layer, 142 °C) is much lower than that of PCM (222 °C), it seems to be an appropriate choice. However, the poor thermal conductivity develops fluid thermal resistance, which depends on the thickness of the fluid layer. Hence, it is important to keep the thickness of the fluid layer as minimum as possible [147].

As mentioned earlier, stiff container walls may be required considering the potential collapse of the system due to buckling if lighter material is employed. However, Pointner et al. [147] have reported that the presence of a fluid layer provides a damping action, and thus, buckling would not be a concern.

6.2.9 Heat Transfer Performance

Unlike other techniques, the PCMflux technique is not investigated from a heat transfer enhancement point of view by the limited number of works reported so far. On the other hand, the PCMflux concept is developed to achieve constant heat flux, especially during the solidification process. To verify the above-mentioned characteristic of the PCMflux concept, a representative module (horizontal version) was tested by Pointner and Steinmann [149], and the results of timewise variation of heat flux are presented in comparison with the stationary case (Fig. 12). In the case of the stationary module, the heat flux was decreasing almost throughout the solidification process. Although a sharp decrease in the heat flux was observed at the beginning and towards the end, the heat flux remained constant during the remaining period in the moving PCM module. In the beginning, the liquid PCM is generally in a

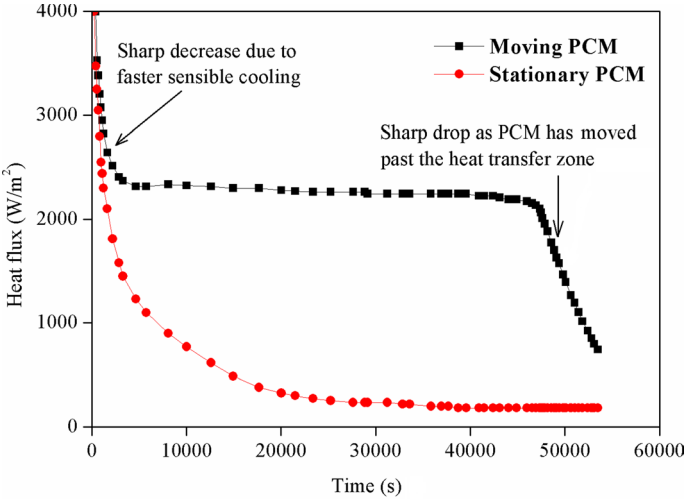

Fig. 12 Timewise variation of heat flux during solidification in moving PCM system and in stationary PCM system [148]

superheated state, and hence, there would be a decrease in heat flux till the sensible heat transfer phase is completed. Further, the sensible cooling process is relatively faster, which causes a sharp decrease in heat flux. As far as the end phase is concerned, the PCM containers have already moved past the heat transfer zone, resulting in a drop in heat flux.

Pointner and Steinmann [149] have further reported a strong relation between the velocity of the containers and the heat flux. The simulation trials have revealed a linear relation between velocity and heat flux up to a particular velocity value, which is called nominal velocity. If a higher than the nominal velocity is used, the PCM moves very fast, reducing the contact time between PCM and HTF. This ultimately results in incomplete phase change. Hence, the system has to be operated at a velocity equal to or below the nominal velocity. It is further mentioned that any value of velocity within the linear variation can exhibit constant heat flux. However, velocities below nominal velocity would result in a quasi-phase change interface even before the container reaches the end of the heat transfer zone. Hence, the heat transfer area is not fully utilized, which means lower values yet constant heat flux would be maintained.

Although minimal experimental and theoretical investigations have been carried out on the PCMflux concept to date, the proof of concept is well demonstrated. In order to make the concept a practically implementable one, future research should focus on the following aspects.

(1) Heat transfer enhancement during melting needs to be investigated.
(2) The extent of heat loss during the travel of containers is not yet reported by any study.

(3) An extensive comparison between a conventional system and a PCMflux system in terms of heat transfer rate, decrease in melting/solidification time, storage/discharge efficiency and energy stored may be carried out.
(4) Considering the questionable durability of aluminum foil, alternative high durable materials may be tested without compromising on cost and thermal conductivity.
(5) Cost analysis should be performed to verify the economic viability of the concept.

6.2.10 Limitations

Similar to other movable PCM systems, systems involving the PCMflux concept also require additional power to operate conveyors. Further, the system seems complex due to the conveyor mechanism, PCM containers and the presence of an intermediate fluid layer.

6.3 Scraping of Solidified Layer

The growing solidified layer of PCM on the heat transfer surface can also be removed with scrapers. Because of the scraping of solid PCM, the heat transfer surface is continuously exposed to liquid PCM, and hence, a nearly constant heat flux condition is achievable. The mechanical scraping of the product of interest is generally required if the heat exchanger handles products that are viscous or sticky or solid–liquid PCMs or possessing solid matter [150]. Hence, this technique is quite popular in industries like chemical, pharmaceutical and food processing. In general, the heat exchangers employing scrapers are known as scraped-surface heat exchangers (SSHX). The SSHXs provide not only high heat transfer rate and nearly constant heat flux but also agitation and mixing of the medium.

6.3.1 Solidification in SSHX

The successful employment of SSHX for enhancing the solidification process is reported in the literature [150–156]. The proposed designs are of two types with respect to the operation of the scrapers. They are.

- Moving scraper
- Fixed scraper or rotating drum

6.3.2 Moving Scraper

In fact, the moving scraper arrangement is widespread in the applications wherein SSHX is employed [150]. In particular, this type is found to be effective in the food industry for the preparation of ice creams, soup, sauce, jam, chocolates, caramels, etc. [157]. A typical movable blade SSHX consists of a centrally located rotating shaft which is provided with two or four pivoted blades. The blades are kept at either

90° or 180° apart, depending on their quantity. The rotating shaft (rotor) with blades is surrounded by a hollow stationary tube that provides space for the product. The product can enter into this space and leave during the processing. The rotor and outer stationary tube are enclosed in another tube so that an annular gap is provided. The HTF is permitted to flow through the annular gap. The construction details of a typical SSHX are presented in Fig. 13.

As the cold HTF flows through the annular gap, the liquid medium in the inner tube starts solidifying on the heat transfer surface. The solidified layer is then removed by the scraper blades, and hence, the liquid medium comes in contact with the heat transfer surface. The blades are generally spring-loaded, and hence, periodical scraping, if required, can be ensured. Using the arrangement explained above, Lakhdar et al. [152] observed enhanced heat transfer characteristics during freezing of water–ethanol mixture. While removing the ice layer formed adjacent to the heat transfer surface, the rotary blades also bring new water solutions available far from the heat transfer surface. This actually reduces the internal thermal resistance contributed by the ice layer formed. Besides removing the ice layer, the rotary blades allow it to mix radially with the rest of the solution. This effect was found to be effective in increasing the freezing rate. By increasing the rotational speed of the blades, the time gap between successive scraping could be reduced. Hence, the reduction in thermal resistance depends on the rotation speed. However, this effect was more pronounced only up to a speed of 500 rpm.

The effect of rotational speed is also addressed by Singh and Kachhwaha [150]. The authors have designed and fabricated a similar configuration for ice slurry production. However, the central tube in which the rotor was placed was wounded by copper coils instead of another single tube enclosure. The copper coils carried the refrigerant, and this acted as an evaporator to produce the cooling effect required for freezing water on the inner heat transfer surface. It is reported that the speed of 24 rpm resulted in the lowest internal thermal resistance of the ice layer. Although Lee et al. [158] have observed the effect of rotational speed on the performance of SSHX, the optimum speed is not reported and rather, the minimum speed of 350 rpm is recommended. Further, the influence of rotational speed was more

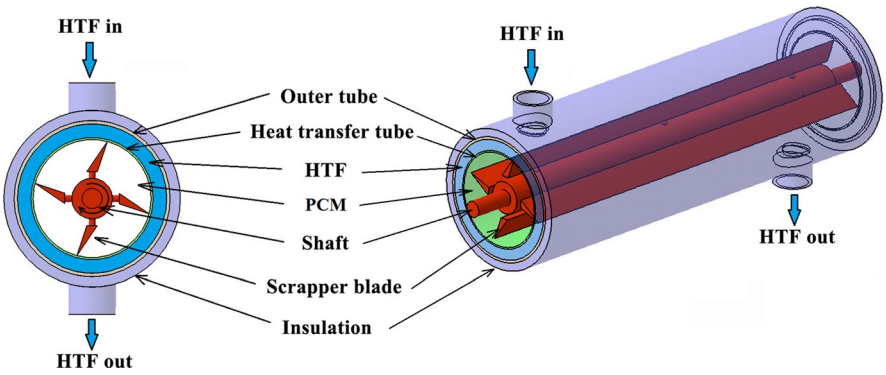

Fig. 13 Schematic of SSHX [157]

pronounced when the flow rate was low. Hence, it is important to optimize the rotational speed of the blades for the lowest possible thermal resistance.

Apart from speed, a couple of parameters pertaining to blades are critical in determining the thermal performance of SSHX. The first parameter in the design is the clearance between the heat transfer surface and the tip of the blades. In fact, if the tip is very close to the surface, the surface would experience mechanical damage. On the other hand, a wide gap between tip and surface is not preferable as it may affect the removal of the solidified layer. Hence, an optimum gap should be identified. According to Lakhdar et al. [152], 1 mm clearance provided effective removal of ice layer without scraping the surface. However, proper coating of the surface is still recommended to avoid potential mechanical damage.

The influence of the shape of the scraper is reported by Baccar and Abid [151]. The authors tested two different shapes. The first one was designed in such a way that the surface of the scraper is perpendicular to the heat transfer surface, whereas it was curved in the case of the second one. As far as heat transfer performance is concerned, the curved one is found to be more effective, although there was a reduction in local heat transfer behind the blades. The authors also investigated the effect of the number of blades. It is obvious that the frequency of removal of the solidified layer increases with an increase in the number of blades. However, the increase in the number of blades also resulted in the expansion of stagnation zones. Further, the heat transfer coefficient enhancement was almost negligible when the number of blades was increased beyond four. It should be noted that the increase in number would increase power consumption. As far as power consumption is concerned, Qin et al. [159] have reported an interesting result. In general, once solidification is initiated, the blades start removing the solidified layer. Hence, it may be expected that the power consumption would increase suddenly as soon as scraping action begins. However, Qin et al. [159] observed that the increase in power consumption was consistent with the increase in a solidified layer rather than a sharp increase at the beginning. As the solid fraction increases, the fluid viscosity tends to increase, which opposes the blades' rotation. Hence power consumption increases with an increase in the solidified layer.

In order to minimize the adverse effect of increased viscous force on blade rotation, Nepustil et al. [153] have proposed linearly moving scrapers. In this design, sliding scrapers were positioned on both the sides of heat exchanger surface. The linear movement of scrapers from one end to the other was done to remove the solidified layer. However, this design did not come out well as the growing layer of solid at the sides reduced the path length of the scrapers. Further, a solid layer reaching the bottom edge of the scraper arrested the scraper movement. Hence, the authors employed a redesigned scraper with a telescopic mechanism and a curved profile at the bottom edge. This design could force the solid layer at the bottom edge to move upward. Hence, the sliding action of the scraper remained unaffected, and ultimately, a higher discharge rate could be achieved. Nevertheless, the design seems to be mechanically complex due to the telescopic mechanism and increased number of supports, frames and bearings.

6.3.3 Fixed scrapers or rotating drum

As the name implies, this design uses fixed scrapers, and the scraping action is achieved by rotating the inner tube which carries the HTF. The use of fixed blades is found to be more effective than moving blades, as the moving blades tend to become ineffective once the solidified layer is formed around the blades [154].

The concept of rotating drum is illustrated in Fig. 14. The HTF flows through the centrally located tube, which is made rotating. The central tube is enclosed by a fixed cylinder which serves as a PCM container. The blades are attached to the inner surface of the PCM container at one edge, and the other edge remains close to the heat transfer surface. The solidified PCM formed on the outer heat transfer surface of the HTF tube is, therefore, removed by the scrapers, which can be easily forced towards the outer end of the PCM container. This ensures the exposure of the heat transfer surface continuously to the liquid PCM. As discussed earlier, the moving scrapers technique has been under research for quite some time now. On the other hand, the rotating drum concept seems to be relatively new, and only few works have reported the outcomes.

Although the pioneering work by Nogami et al. [160] did not consider solid–liquid PCM, the role of rotating drum in increasing the performance during single-phase heat transfer (liquid–liquid) and two-phase heat transfer (liquid–gas) is well demonstrated. The authors have reported a seven-fold increase in overall heat transfer coefficient due to inner tube rotation compared to the conventional double pipe exchanger. Although no scraping of physical material occurred due to a single-phase or liquid–gas medium, the rotation of blades scraped the thermal boundary layer. It is well-known that the thermal boundary layer contributes to the thermal resistance and scraping the boundary layer leads to a reduction in the thermal resistance and hence, enhancement in heat transfer rate. In fact, the authors have recommended employing another set of fixed scrapers inside the rotating tube in order to scrap the inner thermal boundary layer. Double scraping is proved to be more effective than single scraping in enhancing the overall heat transfer coefficient. To the best of authors' knowledge, the one reported by Maruoka et al. [154] is the first attempt employing the rotary drum heat exchanger to enhance the solidification rate of PCM. The authors fabricated a heat exchanger with scrapers on both sides of the

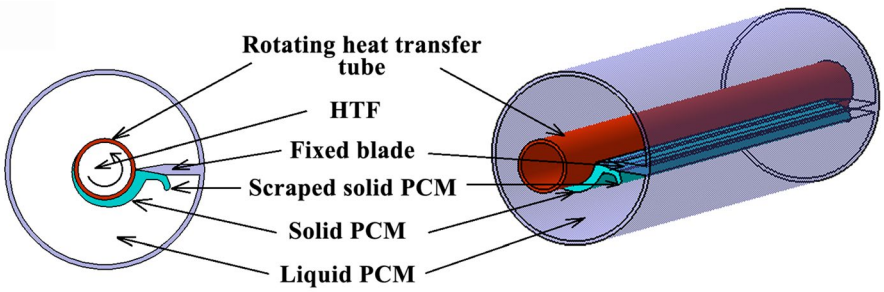

Fig. 14 Schematic of rotating drum heat exchanger [154]

heat transfer surface similar to that proposed by Nogami et al. [160]. The results have revealed a higher heat transfer coefficient due to the rotation of the heat transfer tube. In fact, the overall heat transfer coefficient was found to increase with an increase in rotational speed and the increase was almost 138 times at 500 rpm compared with no rotation case. Besides enhancing the heat transfer rate, the rotation of the tube could enhance the retrieval of energy. Even with low speed (100 rpm), the system could retrieve more than 80 % of latent heat from the PCM in a short period of time (1000 s). On the other hand, even after 4 h, the conventional system could retrieve only 50 % of total latent heat. The amount of energy retrieved increases with an increase in rotational speed.

Following Maruoka et al. [154], Tombrink et al. [155] have proposed a new technique of rotating drum system, and the reported work provides more insights into the heat transfer behavior of PCM under scrapping. In the new design, a rotating drum that carries HTF is immersed in the PCM tank partially. As the drum rotates, the solidified layer formed around the immersed portion of the drum is carried along the container, which reaches the fixed blade located on one side from where it can be removed from the drum. Hence, the scrapping action takes place at each revolution of the drum. Experimentations were performed for three different cases. Besides solidified layer, the rotating drum also carries some quantity of liquid PCM along, and this liquid PCM layer is expected to solidify once the surface of the drum comes out of the container. In the first case, this was investigated, whereas in the second case, the liquid PCM layer carried by the drum was removed using a rubber lip as soon as the drum surface left the liquid PCM. In the first and second cases, the solidified layer reaches the blade only after travelling for some angle of rotation out of the container. However, the scraping of solidified layer shortly after the drum surface came out of the PCM container was considered in the third case. The comparison of the three cases has revealed that an average of 30 % increase in heat transfer is possible in the second case compared to the third one irrespective of the rotational speed. As the drum leaves the liquid PCM, the solidified layer can be further cooled by transferring sensible heat to the surroundings. This would result in additional heat transfer. On the other hand, the first case is found to be more effective as the heat transfer was increased by an average of 45 %. The liquid PCM layer comes out along with the solidified layer tends to solidify prior to reaching the blade. This expands the surface of the active solidified layer, and hence, additional heat transfer is possible. The increase in additional heat transfer was found to be increasing with an increase in rotational speed. Compared to the design proposed by Maruoka et al. [154], the one of Tombrink et al. [155] brings in an additional advantage. The scarped solid PCM can be transferred to a separate storage tank. As discussed already, the separation of heat exchanger and storage tank offers flexibility in heat exchanger design.

The subsequent work by Tombrink et al. [156] has proved that the proposed design is effective for even high-temperature applications. The simulation work on rotating drum heat exchanger having the same geometrical properties as the one employed in Ref. [155], considered a high-temperature PCM (Sodium Nitrate-having a melting temperature of 306 °C). It is shown that the heat transfer coefficient was as high as 6000 $W{\cdot}m^{-2}K$ at 50 rpm, although there was a decrease in the

difference between HTF temperature and the melting point of PCM. Nevertheless, the heat transfer coefficient value was higher than 3000 $W \cdot m^{-2}K$ even when the temperature difference was on the higher side. This value is more than what is generally found in typical evaporators. Hence, the rotating drum heat exchanger seems to have good potential for steam generation in power plants.

6.3.4 Limitations

Basically, SSHX is developed to scrap the thermal boundary layer which exists adjacent to the heat transfer surface. In the systems involving single-phase medium and liquid–gas two-phase medium, it is possible to employ SSHX for both heating and cooling processes. However, for solid–liquid phase change, SHX is proven to be effective only for solidification as the rotating blade or drum may not function effectively in the presence of solid PCM during melting.

As mentioned already, the scraping action may cause mechanical damage to the heat transfer surface. This demands expensive surface coating. In addition to the above disadvantages, the mechanism for moving/rotating the blade/drum adds to the system complexity and cost.

7 Conclusions

The present review focuses on alternative techniques for enhancing phase change heat transfer rate in LHTESS. Although the identified techniques show promising potential in enhancing phase change heat transfer rate without compromising storage capacity, they are not a straightforward solution due to various practical issues. In this perspective, this work evaluates the reported researches on such techniques applicable to LHTESS. The outcomes of this review are summarized as follows.

(1) Direct contact heat exchanger offers a simple configuration as compared to the conventional heat exchanger. However, the clogging of the distribution system by solid PCM crystals and the creation of effective flow channels are the two major issues to be sorted out.
(2) Ultrasonic vibration should not be implemented continuously during the phase change processes; rather, an intermittent operation is recommended.
(3) EHD technique seems to be much simpler than ultrasonic vibration for enhancing the phase change rate.
(4) Although SHX is proved to be effective, the complexity of the system and the cost involved do not work in favor of this technique.
(5) In the PCM recirculation technique, the recirculation lines should be taken care of as they are the major source of heat loss/gain.
(6) The roles of the intermediate fluid layer and the velocity of the PCM container are critical in determining the effectiveness of the PCMflux concept.
(7) For scraping the solidified layer, the rotary drum concept seems better suited than the rotating blade concept.

Declarations

Conflict of interest The authors declare that they have no conflict of interest.

References

1. K. Pielichowska, K. Pielichowski, Prog. Mater. Sci. **65**, 67 (2014)
2. B. Stutz, N. Le Pierres, F. Kuznik, K. Johannes, E. Palomo Del Barrio, J.-P. Bédécarrats, S. Gibout, P. Marty, L. Zalewski, J. Soto, N. Mazet, R. Olives, J.-J. Bezian, D.P. Minh, C. R. Phys. **18**, 401 (2017)
3. Y. Lin, G. Alva, G. Fang, Energy **165**, 685 (2018)
4. R. Zeinelabdein, S. Omer, G. Gan, Renew. Sustain. Energy Rev. **82**, 2843 (2018)
5. Tauseef-ur-Rehman, H. Muhammad Ali, M.M. Janjua, U. Sajjad, W. Yan, Int. J. Heat Mass Transf. **135**, 649 (2019).
6. P. Sivasamy, A. Devaraju, S. Harikrishnan, Mater. Today Proc. **5**, 14423 (2018)
7. C.R. Abujas, A. Jove, C. Prieto, M. Gallas, L.F. Cabeza, Renew. Energy **97**, 434 (2016)
8. Y.B. Tao, Y.L. He, Renew. Sustain. Energy Rev. **93**, 245 (2018)
9. W. Ye, J. Therm. Anal. Calorim. **128**, 533 (2016)
10. Z. Khan, Z. Khan, A. Ghafoor, Energy Convers. Manag. **115**, 132 (2016)
11. S. Pathak, K. Jain, P. Kumar, X. Wang, R.P. Pant, Appl. Energy **239**, 1524 (2019)
12. J. Gasia, J.M. Maldonado, F. Galati, M. De Simone, L.F. Cabeza, Energy Convers. Manag. **184**, 530 (2019)
13. H. Ettouney, I. Alatiqi, M. Al-Sahali, K. Al-Hajirie, Energy Convers. Manag. **47**, 211 (2006)
14. R. Velraj, R.V. Seeniraj, B. Hafner, C. Faber, K. Schwarzer, Sol. Energy **65**, 171 (1999)
15. V. Joshi, M.K. Rathod, J. Energy Storage **22**, 270 (2019)
16. A.H. Sweidan, Y. Heider, B. Markert, Contin. Mech. Thermodyn. **32**, 861 (2019)
17. M. Esapour, A. Hamzehnezhad, A.A. Rabienataj, M. Jourabian, Energy Convers. Manag. **171**, 398 (2018)
18. L. Liu, K. Zheng, Y. Yan, Z. Cai, S. Lin, X. Hu, Sol. Energy Mater. Sol. Cells **185**, 487 (2018)
19. M. Yuan, Y. Ren, C. Xu, F. Ye, X. Du, Renew. Energy **136**, 211 (2019)
20. F. Cheng, Y. Huang, R. Wen, X. Zhang, J. Therm. Anal. Calorim. **136**, 1217 (2019)
21. A.B. Rezaie, M. Montazer, Appl. Energy **228**, 1911 (2018)
22. S. Ebadi, S.H. Tasnim, A.A. Aliabadi, S. Mahmud, Energy Convers. Manag. **166**, 241 (2018)
23. T. Raja Jeyaseelan, N. Azhagesan, V. Pethurajan, J. Therm. Anal. Calorim. **136**, 235 (2019)
24. S.A. Nada, W.G. Alshaer, Heat Mass Transf. **55**, 2667 (2019)
25. S. Jegadheeswaran, S.D. Pohekar, T. Kousksou, Clean: Soil, Air, Water **39**, 964 (2011)
26. L. Klimeš, P. Charvát, M. Ostrý, J. Build. Perform. Simul. **12**, 404 (2019)
27. N. Sheng, C. Zhu, G. Saito, T. Hiraki, M. Haka, Y. Hasegawa, H. Sakai, T. Akiyama, T. Nomura, J. Mater. Chem. A **6**, 18143 (2018)
28. S.M. Sadrameli, F. Motaharinejad, M. Mohammadpour, F. Dorkoosh, Heat Mass Transf. **55**, 1806 (2019)
29. A.F. Regin, S.C. Solanki, J.S. Saini, Renew. Sustain. Energy Rev. **12**, 2438 (2008)
30. S. Höhlein, A. König-Haagen, D. Brüggemann, Materials (Basel) **11**, 1752 (2018)
31. P.K.S. Rathore, S.K. Shukla, Constr. Build. Mater. **225**, 723 (2019)
32. D. Vérez, E. Borri, A. Crespo, B.D. Mselle, Á. de Gracia, G. Zsembinszki, L.F. Cabeza, Appl. Sci. **11**, 6171 (2021)
33. A.K. Raj, M. Srinivas, S. Jayaraj, Appl. Therm. Eng. **146**, 910 (2019)
34. F. Ahmed, M. Mahmood, A. Waqas, N. Ahmad, M. Ali, Sustain. Energy Technol. Assess. **47**, 101533 (2021)
35. N. Beemkumar, A. Karthikeyan, D. Yuvarajan, S. Lakshmi Sankar, Arab. J. Sci. Eng. **42**, 2055 (2017)
36. N. Lakshmi Narasimhan, J. Energy Storage **23**, 442 (2019)
37. G. Peiro, J. Gasia, L. Miro, L.F. Cabeza, Renew. Energy **83**, 729 (2015)
38. S. Jegadheeswaran, S.D. Pohekar, Renew. Sustain. Energy Rev. **13**, 2225 (2009)
39. L. Liu, D. Su, Y. Tang, G. Fang, Renew. Sustain. Energy Rev. **62**, 305 (2016)

40. N.I. Ibrahim, F.A. Al-sulaiman, S. Rahman, B.S. Yilbas, A.Z. Sahin, Renew. Sustain. Energy Rev. **74**, 26 (2017)
41. Z.A. Qureshi, H.M. Ali, S. Khushnood, Int. J. Heat Mass Transf. **127**, 838 (2018)
42. R. Elarem, T. Alqahtani, S. Mellouli, F. Askri, A. Edacherian, T. Vineet, I.A. Badruddin, J. Abdelmajid, Energy Storage **3**, e127 (2020)
43. S. Jegadheeswaran, A. Sundaramahalingam, S.D. Pohekar, J. Therm. Anal. Calorim. **138**, 1137 (2019)
44. N.H.S. Tay, M. Liu, M. Belusko, F. Bruno, Renew. Sustain. Energy Rev. **75**, 264 (2017)
45. R.F. Boehm, F. Krieth, *Direct-Contact Heat Transfer Process* (Springer, Berlin, 1988), pp. 1–24
46. S. Kunkel, T. Teumer, P. Dörnhofer, F. Wunder, J.U. Repke, M. Rädle, J. Energy Storage **28**, 101178 (2020)
47. R. Elbahjaoui, H. El Qarnia, Energy Build. **182**, 111 (2019)
48. J. Duan, Y. Liu, L. Zeng, Y. Wang, Q. Su, J. Wang, ACS Omega **6**, 13601 (2021)
49. L. Miró, J. Gasia, L.F. Cabeza, Appl. Energy **179**, 284 (2016)
50. S. Das, A. Biswas, B. Das, in *Advanced Mechanical Engineering ICRAME 2020*, ed. by K. M. Pandey, R. D. Misra, P. K. Patowari, U. S. Dixit (Springer, Singapore, 2020).
51. W.P. Missana, E. Park, T.T. Kivevele, J. Energy **2020**, 9205283 (2020)
52. T.L. Etherington, Heat. Pip. Air Cond. **29**, 147 (1957)
53. D. D. Edie, S. S. Melsheimer, J. C. Mullins, in *Proceedings of the International Conference* (Winnipeg, 1976), pp. 391–399.
54. D.D. Edie, C.G. Sandell, L.E. Kizer, J.C. Mullins, in *Proceedings of the Annual Meeting—American Section of the International Solar Energy Society* (1977), pp. 26–30.
55. V. Costello, S. S. Melsheimer, and D. D. Edie, in *Winter Annual Meeting The American Society of Mechanical Engineers* (San Francisco, 1978), pp. 51–60.
56. B. He, F. Setterwall, Energy Convers. Manag. **43**, 1709 (2002)
57. V. Martin, B. He, F. Setterwall, Appl. Energy **87**, 2652 (2010)
58. X.Y. Li, Q.Q. Zhao, D.Q. Qu, Appl. Therm. Eng. **91**, 172 (2015)
59. T. Kiatsiriroat, S. Vithayasai, N. Vorayos, A. Nuntaphan, N. Vorayos, Energy Convers. Manag. **44**, 497 (2003)
60. P. Mulyono, Energy **29**, 2573 (2004)
61. A. Horibe, H. Jang, N. Haruki, Y. Sano, H. Kanbara, K. Takahashi, Int. J. Heat Mass Transf. **82**, 259 (2015)
62. T.T. Naing, A. Horibe, N. Haruki, Y. Yamada, J. Power Energy Eng. **05**, 13 (2017)
63. M. Belusko, S. Sheoran, F. Bruno, Appl. Energy **137**, 748 (2015)
64. A.E. Fouda, G.J.G. Despault, J.B. Taylor, C.E. Capes, Sol. Energy **25**, 437 (1980)
65. A.E. Fouda, G.J.G. Despault, J.B. Taylor, C.E. Capes, Sol. Energy **32**, 57 (1984)
66. T. Kiatsiriroat, J. Tiansuwan, T. Suparos, K.N. Thalang, Renew. Energy **20**, 195 (2000)
67. S. Kunkel, T. Teumer, P. Dörnhofer, K. Schlachter, Y. Weldeslasie, M. Kühr, M. Rädle, J. Repke, Appl. Therm. Eng. **145**, 71 (2018)
68. T. Nomura, M. Tsubota, N. Okinaka, T. Akiyama, ISIJ Int. **55**, 441 (2015)
69. T. Nomura, M. Tsubota, A. Sagara, N. Okinaka, T. Akiyama, Appl. Therm. Eng. **58**, 108 (2013)
70. M.M. Farid, K. Yacoub, Sol. Energy **43**, 237 (1989)
71. M.M. Farid, A.N. Khalaf, Sol. Energy **52**, 179 (1994)
72. T. Nomura, M. Tsubota, T. Oya, N. Okinaka, T. Akiyama, Appl. Therm. Eng. **50**, 26 (2013)
73. T. Nomura, M. Tsubota, T. Oya, N. Okinaka, T. Akiyama, Appl. Therm. Eng. **61**, 28 (2013)
74. S. Guo, H. Li, J. Zhao, X. Li, J. Yan, Appl. Energy **112**, 1416 (2013)
75. W. Wang, S. Guo, H. Li, J. Yan, J. Zhao, X. Li, J. Ding, Appl. Energy **119**, 181 (2014)
76. W. Wang, S. He, S. Guo, J. Yan, J. Ding, Energy Convers. Manag. **83**, 306 (2014)
77. W. Wang, H. Li, S. Guo, S. He, J. Ding, J. Yan, J. Yang, Appl. Energy **150**, 61 (2015)
78. W. Wang, *Mobilized Thermal Energy Storage for Heat Recovery for Distributed Heating* (Mälardalen University, Sweden, 2010)
79. S. Guo, J. Zhao, W. Wang, G. Jin, X. Wang, Q. An, W. Gao, Appl. Therm. Eng. **78**, 556 (2015)
80. L. Gao, J. Zhao, Q. An, D. Zhao, F. Meng, X. Liu, Appl. Therm. Eng. **113**, 858 (2017)
81. W. Wang, S. He, J. Ding, H. Li, J. Yan, J. Yang, Energy Procedia **105**, 4389 (2017)
82. A.S. Sowayan, J. Comput. Theor. Nanosci. **19**, 889 (2013)
83. L. Zhang, J. Lv, M. Bai, D. Gou, Heat Transf. Eng. **36**, 452 (2015)
84. A. Hosseinian, A.H.M. Isfahani, E. Shirani, Exp. Therm. Fluid Sci. **90**, 275 (2018)
85. N. Kozlov, Shock Vib. **2019**, 1 (2019)

86. W. Liu, Z. Yang, B. Zhang, P. Lv, Int. J. Heat Mass Transf. **115**, 169 (2017)
87. A. Hosseinian, A.H.M. Isfahani, Heat Mass Transf. **54**, 1113 (2018)
88. M. Hajiyan, M. Al-jethelah, Y. Alomair, M. Alomair, S. Tasnim, S. Mahmud, in *Proceedings of the 5th International Conference of Fluid Flow, Heat and Mass Transfer* (Niagara Falls, Canada, 2018), pp. 190–198.
89. L. Quan, *Contact Melting of Phase Change Material with Effect of Vibration* (University of Rhode Island, Kingston, 1999)
90. A. Shirvanian, M. Faghri, Z. Zhang, Y. Asako, Numer. Heat Transf. Part A Appl. Int. J. Comput. Methodol. **34**, 257 (1998)
91. M. Oka, *Advances in Cold-Region Thermal Engineering and Sciences: Lecture Notes Physics* (Springer, Berlin, 1999), pp. 91–102
92. I. Raben, in *Proceedings of the Heat Transfer and Fluid Mechanics Institute* (Los Angeles, CA, 1961), pp. 90–97.
93. M. Legay, N. Gondrexon, S. Le Person, P. Boldo, A. Bontemps, Int. J. Chem. Eng. **2011**, 1 (2011)
94. S. Sutariya, V. Sunkesula, R. Kumar, K. Shah, Cogent Food Agric. **4**, 1 (2018)
95. R. Manasseh, *Handbook of Ultrasonics and Sonochemistry* (Springer, Singapore, 2016), pp. 33–67
96. H. V. Fairbanks, in *1979 Ultrasonics Symposium* (New Orleans, LA, 1979), pp. 384–387.
97. K.J. Choi, J.S. Hong, J. Thermophys. **5**, 340 (1991)
98. Y.K. Oh, S.H. Park, K.O. Cha, KSME Int. J. **15**, 1882 (2001)
99. J.J. Vadasz, J.P. Meyer, S. Govender, G. Ziskind, Exp. Heat Transf. **29**, 285 (2016)
100. F. Baillon, F. Espitalier, C. Cogné, R. Peczalski, O. Louisnard, *Power Ultrasonics* (Woodhead Publishing, Sawston, 2014)
101. L. Zhegg, D.-W. Sun, *Emerging Technologies for Food Processing* (Elsevier, London, 2005), pp. 603–626
102. Z. Zhang, D.W. Sun, Z. Zhu, L. Cheng, Compr. Rev. Food Sci. Food Saf. **14**, 303 (2015)
103. L. Wei, K. Ohsasa, ISIJ Int. **50**, 1265 (2010)
104. F. Hu, D.W. Sun, W. Gao, Z. Zhang, X. Zeng, Z. Han, Innov. Food Sci. Emerg. Technol. **20**, 161 (2013)
105. H. Feng, W. Yang, T. Hielscher, Food Sci. Technol. Int. **14**, 433 (2008)
106. A. Mulet, J. Benedito, J. Bon, N. Sanjuan, Food Sci. Technol. Int. **5**, 285 (1999)
107. Y.K. Oh, S.H. Park, Y.I. Cho, Int. J. Heat Mass Transf. **45**, 4631 (2002)
108. Y.K. Oh, H.D. Yang, Key Eng. Mater. **324–325 II**, 1075 (2006)
109. H.D. Yang, Y.K. Oh, Int. J. Mod. Phys. B **20**, 4341 (2006)
110. N. Zhang, Y. Du, Sustain. Cities Soc. **43**, 532 (2018)
111. D. Nakhla, H. Sadek, J.S. Cotton, Int. J. Heat Mass Transf. **81**, 695 (2015)
112. Y. Guan, R.S. Vaddi, A. Aliseda, I. Novosselov, Phys. Rev. Fluids **3**, 043701 (2018)
113. M. Rezaee, A.A. Taheri, M. Jafari, Int. Commun. Heat Mass Transf. **119**, 104969 (2020)
114. P.H.G. Allen, T.G. Karayiannis, Heat Recover. Syst. CHP **15**, 389 (1995)
115. J.E. Bryan, J. Seyed-Yagoobi, J. Heat Transf. **123**, 355 (2001)
116. H. Sadek, A.J. Robinson, J.S. Cotton, C.Y. Ching, M. Shoukri, Int. J. Heat Mass Transf. **49**, 1647 (2006)
117. G. McGranaghan, A.J. Robinson, Heat Transf. Eng. **35**, 517 (2014)
118. P.R. Dellorusso, *Electrohydrodynamic Heat Transfer Enhancement for a Latent Heat Storage Heat Exchanger* (Technical University of Nova Scotia, Halifax, 1997)
119. D. Nakhla, E. Thompson, B. Lacroix, J.S. Cotton, J. Electrostat. **92**, 31 (2018)
120. D. Nakhla, J.S. Cotton, Int. J. Heat Mass Transf. **167**, 120828 (2021)
121. R.D. Selvakumar, L. Qiang, L. Kang, P. Traoré, J. Wu, Int. J. Multiph. Flow **136**, 103550 (2021)
122. K. Luo, A.T. Pérez, J. Wu, H.L. Yi, H.P. Tan, Phys. Rev. E **100**, 013306 (2019)
123. Z. Sun, P. Yang, K. Luo, J. Wu, Int. J. Heat Mass Transf. **173**, 121238 (2021)
124. J. Gasia, N.H.S. Tay, M. Belusko, L.F. Cabeza, F. Bruno, Appl. Energy **185**, 136 (2017)
125. B. Janowska, P. Regucki, A. Andruszkiewicz, W. Wędrychowicz, in *E3S Web Conf.* (2017), pp. 4–11
126. A. Mustaffar, A. Phan, K. Boodhoo, Chem. Eng. Process. Process. Intensif. **128**, 199 (2018)
127. S.S. Waje, B.N. Thorat, A.S. Mujumdar, Dry. Technol. **24**, 293 (2006)
128. M. Yadav, O. Patil, A. Salunge, M. Kulkarni, V. Diware, Int. J. Eng. Sci. Comput. **7**, 4420 (2017)
129. O. Kaplan, C. Celik, Fuel **215**, 468 (2018)
130. M. Cucumo, V. Ferraro, D. Kaliakatsos, F. Crea, F. Tassone, A. Mumoli, M. Mele, Int. J. Heat Technol. **35**, S427 (2017)

131. S.H. Teo, H.L. Gan, A. Alias, L.M. Gan, IOP Conf. Ser. Mater. Sci. Eng. **342**, 012096 (2018)
132. P. Andersen, AIP Conf. Proc. **791**, 1–6 (2015)
133. C.I. Chung, *Extrusion of Polymers-Theory and Practice*, 2nd edn. (Hanser Publishers, Minich, 2019)
134. S.V. Ershov, N.M. Trufanova, I.O.P. Conf, Ser. Mater. Sci. Eng. **208**, 1 (2017)
135. H. He, J.Y. He, Y. Liu, Adv. Mater. Res. **941–944**, 1769 (2014)
136. V. Zipf, A. Neuhäuser, D. Willert, P. Nitz, S. Gschwander, W. Platzer, Appl. Energy **109**, 462 (2013)
137. V. Zipf, A. Neuhäuser, C. Bachelier, R. Leithner, W. Platzer, Energy Procedia **69**, 1078 (2015)
138. V. Zipf, D. Willert, A. Neuhäuser, AIP Conf. Proc. **1734**, 050044 (2016)
139. V. Zipf, D. Willert, A. Neuhauser, *Dynamic Concept at Fraunhofer* (Elsevier Ltd, Amsterdam, 2017)
140. N. H. S. Tay, M. Belusko, F. Bruno, in *12th International Conference on Energy Storage* (Lleida, 2012), pp. 1–10.
141. N.H.S. Tay, F. Bruno, M. Belusko, Appl. Energy **104**, 137 (2013)
142. N.H.S. Tay, M. Belusko, M. Liu, F. Bruno, Appl. Energy **137**, 738 (2015)
143. J. Gasia, D. Groulx, N.H.S. Tay, L.F. Cabeza, J. Energy Storage **31**, 101664 (2020)
144. H. Pointner, W. D. Steinmann, in *IEA-ECES Greenstock 2015* (Peking, China, 2015).
145. W.D. Steinmann, *Dynamic Concept at German Aerospace Center* (Elsevier Ltd, Amsterdam, 2018)
146. H. Pointner, W.-D. Steinmann, M. Eck, in *Eurotherm Semin. #99 Adv. Therm. Energy Storage*, ed. by L. F. Cabeza and G. Ziskind (Lleida, 2014), p. 8.
147. H. Pointner, W.D. Steinmann, M. Eck, C. Bachelier, Energy Procedia **69**, 997 (2015)
148. H. Pointner, W.D. Steinmann, M. Eck, Energy Procedia **57**, 643 (2014)
149. H. Pointner, W.D. Steinmann, Appl. Energy **168**, 661 (2016)
150. R. Singh, S.S. Kachhwaha, Int. J. Eng. Sci. Innov. Technol. **2**, 117 (2013)
151. M. Baccar, M.S. Abid, Rev. Gén. Therm. **36**, 782 (1997)
152. M. Ben Lakhdar, R. Cerecero, G. Alvarez, J. Guilpart, D. Flick, A. Lallemand, Appl. Therm. Eng. **25**, 45 (2005)
153. U. Nepustil, D. Laing-Nepustil, D. Lodemann, R. Sivabalan, V. Hausmann, Energy Procedia **99**, 314 (2016)
154. N. Maruoka, T. Tsutsumi, A. Ito, M. Hayasaka, H. Nogami, Energy **205**, 118055 (2020)
155. J. Tombrink, H. Jockenhöfer, D. Bauer, Appl. Therm. Eng. **183**, 116221 (2021)
156. J. Tombrink, D. Bauer, Appl. Therm. Eng. **194**, 117029 (2021)
157. A.A.T. Smith, S.K. Wilson, B.R. Duffy, N. Hall-Taylor, J. Eng. Math. **68**, 301 (2010)
158. H.K. Lee, K.H. Choi, J.I. Yoon, C.G. Moon, M.J. Jeon, J.H. Lee, K.S. Lee, C.H. Son, Appl. Sci. **8**, 2063 (2018)
159. F. Qin, X.D. Chen, S. Ramachandra, K. Free, Sep. Purif. Technol. **48**, 150 (2006)
160. H. Nogami, K. Aonuma, Y. Chiba, ISIJ Int. **50**, 1276 (2010)

Authors and Affiliations

Selvaraj Jegadheeswaran[1] · Athimoolam Sundaramahalingam[2] · Sanjay D. Pohekar[3]

Athimoolam Sundaramahalingam
sundaramahalingama@bitsathy.ac.in

Sanjay D. Pohekar
sdpohekar@gmail.com

[1] Academics, Research and Development, Bannari Amman Institute of Technology, Sathyamangalam, Erode 638401, India

[2] Department of Mechanical Engineering, Bannari Amman Institute of Technology, Sathyamangalam, Erode 638401, India

[3] Symbiosis Center for Research and Innovation, Symbiosis International (Deemed University), Lavale, Pune 412115, India